



Dehaene, Vinckier, Jobert, & Montavont, 2008; Price, Wise, & Frackowiak, 1996).

Most of the world's reading systems make use of visual symbols, and most of what we know about the neural basis of reading concerns visual reading. By contrast, braille is a distinctive tactile orthographic system used primarily by blind and visually impaired readers whose neural bases are still poorly understood. Braille is read by passing the fingers across a raised dot array. Each braille symbol, called a "cell," is constructed out of six possible dot positions arranged in a 3 (horizontal) × 2 (vertical) array. Apart from being tactile, braille differs from print in that it consists of disconnected dots and therefore lacks lines or line junctions, which have been noted as a universal property of visual scripts (Chang et al., 2015; Dehaene, Cohen, Sigman, & Vinckier, 2005). Although raised print letters with lines were in use in 18th and 19th century, braille proved to be a more efficient tactile reading code and has been universally adopted by blind communities all over the world after its invention by a blind 15-year-old student, Louis Braille in 1829.

The form of Braille most commonly used by English-speaking proficient blind readers is called Contracted Unified English Braille (UEB; Simpson, 2013). Contracted UEB contains 26 cells designated to represent each Roman letter of the English alphabet (e.g., "⠁" represents "a," "⠃" represents "b," and "⠵" stands for "z"). However, some Roman letter combinations are represented with strings of one or more braille cells called "contractions." The number of braille cells in a contraction is always less than the number of Roman letters it represents. For example, "ing" is represented with a single cell "⠇," "er" is represented with another single cell "⠑," and the string "one-" in the word "honey" (⠁ ⠃ ⠇) is represented by a two-cell contraction "⠁⠃." These are examples of contractions with their own braille cells or cell combinations, whereas other contractions may be represented by multipurpose single cells that serve to represent either a single letter or a word, depending on the context. For example, ⠄ stands for the letter "h" when it is part of a word like "happy" (⠁ ⠃ ⠇ ⠄), but when presented alone, it stands for the word "have." Because contractions stand for frequent letter combinations and/or words, they are an important part of naturalistic English braille reading.

Proficient English-speaking readers most frequently use contracted braille to read, and for writing in braille directly on a Perkins brailler or a smartphone. Proficient braille readers are faster to read contracted versions of frequent words than their uncontracted, letter-by-letter spelled-out counterparts (e.g., "s-u-g-ar" contracted ⠠⠎⠤⠠⠠⠠; uncontracted ⠠⠎⠤⠠⠠⠠ ⠠⠠⠠, "s-u-g-a-r"; Millar, 1997). However, blind English-speakers learn the spellings of words in the uncontracted (i.e., Roman letter) English alphabet as well as the contracted forms of words and the contraction rules (Millar, 1997). Uncontracted spellings are typically used when writing on a computer keyboard or when spelling out loud. Proficient English braille readers thus know

and use two orthographic codes for spelling in braille: contracted and uncontracted.

There is evidence that the uncontracted spellings influence processing, even when reading contracted forms. When contractions interrupt the sublexical structure of the uncontracted wordform, they slow down braille reading. That is, contractions that span across boundaries of sublexical units such as morphemes (e.g., ⠠⠠⠠⠠⠠⠠, **r-en-e-w**) are read more slowly than contractions that do not interrupt morphemes (e.g., ⠠⠠⠠⠠⠠⠠, **en-t-r-y**; Fischer-Baum & Englebretson, 2016). This finding is analogous to what has been reported for print reading, where it takes longer to read a word if it has been artificially segmented in a way that violates the boundaries of the sublexical linguistic units, than if the segmenting does not violate those units (e.g., for French readers, segmenting the word "champignon" in to "ch-am-p-i-gn-on" is easier to read than "c-ha-mp-ig-no-n"; Bouhali, Bézagu, Dehaene, & Cohen, 2019; Rapp, 1992; Prinzmetal, Treiman, & Rho, 1986). How contractions influence the neural processing of Braille words has not previously been tested.

The distinctive nature of braille as a writing system makes understanding its neural basis of particular interest, yet much remains unknown about how braille is neurally implemented. Previous studies have identified a wide network of areas that are active while reading braille but how specific cognitive processes that support braille reading are implemented remains uncertain. The anatomical location of the VWFA, which is important for letter and word recognition in visual print reading, is also active during braille reading (Raczy et al., 2019; Burton, Sinclair, & Agato, 2012; Reich, Szwed, Cohen, & Amedi, 2011; Büchel, Price, & Friston, 1998; Sadato et al., 1998). However, whether the VWFA supports similar or different cognitive processes for braille and visual prints is not known. The VWFA location has been shown more responsive to speech and high-level linguistic information (e.g., grammatical complexity of spoken sentences) in blind than in sighted individuals, although some responses to spoken language in this region have also been observed in the sighted (Tian, Saccone, Kim, Kanjlia, & Bedny, 2022; Dzięciel-Fivet et al., 2021; Kim, Kanjlia, Merabet, & Bedny, 2017). Braille reading also engages many other occipital regions besides the vOTC, including primary visual (V1) and dorsal occipital cortices (Burton et al., 2012; Burton, Diamond, & McDermott, 2003; Burton, Snyder, Diamond, & Raichle, 2002; Büchel et al., 1998; Sadato et al., 1998).

Braille reading also engages the PPC/parieto-occipital cortices, which are implicated in high-level tactile perception (Burton et al., 2002, 2003, 2012; Büchel et al., 1998; Sadato et al., 1998). Although the PPC is sometimes reported in studies of visual reading (Vogel et al., 2013; Vogel, Miezin, Petersen, & Schlaggar, 2012; Ischebeck et al., 2004; Jobard, Crivello, & Tzourio-Mazoyer, 2003), responses in this region to braille are more extensive and more selective for written words (Tian et al., 2022).

Moreover, the lateralization of responses to braille words in PPC of blind readers is also suggestive of a reading-related orthographic role, because it is influenced not only by reading hand (right or left) but also by spoken language lateralization (Tian et al., 2022).

Which, if any, of the cortical areas responsive to braille specifically support reading-specific form-based orthographic processes, as opposed to tactile discrimination and semantic processing, remains unclear. Most prior studies have compared braille reading to low-level control conditions that differ from braille in somatosensory and linguistic properties, and these studies have relied exclusively on univariate analyses (Raczy et al., 2019; Kim et al., 2017; Burton et al., 2012). The objective of the current experiment was to look for neural signatures of reading-specific, form-based orthographic processing during reading of single braille words. We aimed to separate these processes from low-level somatosensory process on the one hand, and high-level language (e.g., semantic) processing on the other, using univariate and multivariate analytic approaches.

To distinguish orthographic from lower-level tactile processes, we first leveraged contractions present in English braille. Despite contractions being a major part of naturalistic English braille reading, to our knowledge, no prior study has examined neural responses to them. The existence of contractions makes it possible to study effects of length of uncontracted orthographic forms on neural activity, while holding the number of cells, and thus low-level tactile features, constant. For example, the words “c-o-r-n” (⠠⠠⠠⠠) and “con-c-er-t” (⠠⠠⠠⠠) are identical in numbers of braille cells, (i.e., both are four cells long) but their corresponding uncontracted forms differ in length (i.e., “concert” is seven while “corn” is four letters long because the former has two contractions). We reasoned that cortical areas involved in orthographic processing would show sensitivity to the length of the underlying uncontracted forms of words, even when the number of cells in the contracted form is held constant.

We hypothesized that uncontracted word length would influence neural activity in PPCs. PPC is a candidate location for braille orthographic processes because of its involvement in high-level tactile perception and has been implicated in braille reading by prior studies (Burton et al., 2002, 2003, 2012; Büchel et al., 1998; Sadato et al., 1998). A recent study also found evidence for an anterior to posterior braille reading gradient, from S1 to PPC in blind readers (Tian et al., 2022). We therefore predicted that uncontracted word length would affect activity in the PPC posterior to S1.

On the other hand, to look for low-level tactile effects, we quantified the amount of somatosensory stimulation in a given word by counting the number of raised dots. A letter like “a” (⠁) consists of one dot, whereas “y” (⠽) has five. This physical property of letters is orthogonal to orthography because each letter stands for a unique grapheme, regardless of its dot count. We predicted that

words with a greater number of dots, and thus greater tactile stimulation, would be associated with greater activity in the hand region of early somatosensory cortex S1, but not the PPC.

We also investigated the effect of word frequency on neural activity in braille reading. Less frequent visual and braille words are read more slowly, providing a basis for a neural signature of frequency in braille (Brybaert, Mander, & Keuleers, 2018; Millar, 1997; Monsell, Doyle, & Haggard, 1989). In sighted readers, frequency affects neural activity in different cortical networks than those affected by word length (in Roman letters [Woolnough et al., 2021; Lin, Yu, Zhao, & Zhang, 2016; Rapp, Purcell, Hillis, Capasso, & Miceli, 2016; Schuster, Hawelka, Hutzler, Kronbichler, & Richlan, 2016; Dehaene & Cohen, 2011; Rapp & Dufor, 2011; Kronbichler et al., 2004; Kuo et al., 2003]). We hypothesized that the same would be true for braille.

To test these predictions, we asked congenitally blind participants to read single braille words and pseudowords. To ensure attentive reading, we asked participants to carry out a dual lexical decision and semantic judgment task. Participants judged if braille stimuli corresponded to a pseudoword, or an animate/inanimate real word. Lexical decision tasks have been widely used in behavioral and neuroimaging studies of reading (Fischer-Baum, Bruggemann, Gallego, Li, & Tamez, 2017; Wang, Zhao, Zevin, & Yang, 2016; Cohen et al., 2008; Ischebeck et al., 2004; Goswami, Ziegler, Dalton, & Schneider, 2001; Coltheart, Patterson, & Leahy, 1994; Van Orden, Johnston, & Hale, 1988). Compared with passive viewing and repetition detection, lexical decision requires more attentive orthographic analysis and recall from the orthographic long-term memory (the orthographic lexicon). The addition of a semantic judgment ensured that participants were also reading for meaning. The uncontracted length of words in the experiment was unrelated to the experimental tasks, because both types of real words and pseudowords contained contractions.

A secondary goal of the current study was to compare reading of braille words to braille pseudowords. In the case of visual print reading, previous studies found that particularly during slow-presentation tasks, form-based (orthographic and phonological) cortical networks respond more to pseudowords than to real words (Bouhali et al., 2019; Taylor, Rastle, & Davis, 2013; Mano et al., 2012; Liu et al., 2008; Dietz, Jones, Gareau, Zeffiro, & Eden, 2005; Hagoort et al., 1999). By contrast, even in attentionally demanding tasks, cortical areas involved in semantic processing respond more to meaningful words than pseudowords (Protopapas et al., 2016; Taylor et al., 2013; Hagoort et al., 1999; Price et al., 1996). We predicted that cortical areas sensitive to orthographic form in braille, and, in particular, orthographic processing of sublexical units (e.g., letters and letter groups), would respond more to pseudowords than real words during braille reading, whereas cortical areas involved in semantic processing

would respond more to real words than pseudowords (Kronbichler et al., 2004; Mechelli, Gorno-Tempini, & Price, 2003).

In addition, we used multivariate pattern analysis (MVPA) to identify cortical networks whose patterns of activity differentiate real and pseudowords, even once univariate signal differences are controlled. To our knowledge, no prior studies have used an MVPA classification approach to examine orthographic/lexical information in patterns of activity during braille reading. Instead of asking whether each single voxel or vertex in the brain is more active in some condition than others, MVPA allows us to ask whether patterns of activity within a cortical area are sensitive to the lexical status of braille stimuli (Haxby, Connolly, & Guntupalli, 2014; Norman, Polyn, Detre, & Haxby, 2006). Even if a cortical area is involved in processing both real and pseudowords to a similar degree, as measured by univariate responses, multivariate patterns may pick up on distinctive processes and/or representations engaged by real and pseudowords. Areas showing the following three effects: sensitivity to uncontracted word length, univariate sensitivity to pseudowords compared with words, and multivariate differences between pseudo and real words are particularly good candidates for important neural circuits involved in form-based orthographic processing of braille.

A third objective of this project was to attempt, for the first time, to detect unique neural signatures of individual braille words. Because braille reading is a tactile, temporally extended process, this may pose special challenges for fMRI-based analysis. Our approach and exploratory findings on this issue may advise future studies on braille reading.

## METHODS

### Participants

Twelve congenitally blind native English speakers (six women,  $M = 39.5$  years of age,  $SD = 11.3$  years, range = 21–64 years) participated in the study. All of the participants were fluent braille readers who began learning braille in early childhood ( $M = 4.3$  years of age,  $SD = 1.5$  years). Because proficient blind braille readers are a small population, we compensated for the relatively small number of participants by collecting a large amount of data per participant (i.e., 1 hr 45 min of functional braille reading data per person). The behavioral data and the motion parameters suggest that we obtained a large quantity of high-quality data from each of our participants. The sample size of the current study is within the range of previous studies with this population (Vetter et al., 2020; Kim et al., 2017; Striem-Amit et al., 2015; Peelen, He, Han, Caramazza, & Bi, 2014).

All of the participants had at most minimal light perception since birth and blindness because of pathology anterior to the optic chiasm (see Table 1 for the cause of

**Table 1.** Participant Information

<i>Blindness Etiology</i>	<i>n</i>
Leber congenital amaurosis	5
Retinopathy of prematurity	4
Born without optic nerve	1
Optic nerve detached	1
Unknown retinal defect	1

blindness). Participants were screened for cognitive and neurological disabilities through self-report. The structural images of the participants were inspected by radiologists in Johns Hopkins Hospital, and no gross neurological pathologies were detected. Participants gave informed consent and were compensated \$30 per hour. All procedures were approved by the Johns Hopkins Medicine institutional review board.

### Stimuli and Task

We chose a dual task procedure to ensure that participants were attending both to the orthography and the meaning of the words. Participants read real words and pseudowords presented on an MRI-compatible refreshable braille and tactile graphic display (Piezoelectric Tactile Stimulus Device developed by KGS Corporation, Japan; see Bauer et al. [2015]). The braille display consisted of an array of 32 by 35 pins (spaced 2.4 mm apart). On each trial, a braille word/pseudoword was displayed for 3 sec followed by a 3-sec blank. Participants pressed one of three buttons to indicate whether the presented word was an inanimate real word, an animate real word, or a pseudoword. They were instructed to make a response as soon as they knew the answer.

Real words consisted of inanimate words (e.g., corn,  $n = 30$ ) and animate words (e.g., dancer,  $n = 30$ ) selected from the top 20,000 most frequent words in the Corpus of Contemporary American English (Davies [2008]; <https://www.english-corpora.org/coca/>; see Table 2 for stimuli). Pseudowords ( $n = 30$ ) were created by retaining the first two cells of an inanimate real word and replacing the last two cells with other braille cells, including cells that stand for contractions. For example, the real word ⠠⠠⠠⠠⠠⠠ (con-v-e-y) was modified to create the pseudoword ⠠⠠⠠⠠⠠⠠ (con-v-u-k). Before the fMRI experiment, we asked a braille reader to read aloud the pseudowords and confirm that all of them were pronounceable (see Table 2 for stimuli).

To our knowledge, no prior study has done MVPA with braille, a dynamic tactile reading system. Because we intended to conduct an MVPA with braille reading neuroimaging data, we tried to have as many repetitions as possible for at least one of the word categories to get the most

**Table 2.** List of Stimuli Words and Their Braille Transcriptions

<i>Inanimate Real Words</i>					
bread	⠠⠠⠠⠠	cereal	⠠⠠⠠⠠	chess	⠠⠠⠠⠠
choir	⠠⠠⠠⠠	concert	⠠⠠⠠⠠	convey	⠠⠠⠠⠠
corn	⠠⠠⠠⠠	eight	⠠⠠⠠⠠	elbow	⠠⠠⠠⠠
exert	⠠⠠⠠⠠	fewer	⠠⠠⠠⠠	five	⠠⠠⠠⠠
foot	⠠⠠⠠⠠	forearm	⠠⠠⠠⠠	grain	⠠⠠⠠⠠
half	⠠⠠⠠⠠	honey	⠠⠠⠠⠠	jazz	⠠⠠⠠⠠
knee	⠠⠠⠠⠠	milk	⠠⠠⠠⠠	opera	⠠⠠⠠⠠
seven	⠠⠠⠠⠠	single	⠠⠠⠠⠠	sugar	⠠⠠⠠⠠
sway	⠠⠠⠠⠠	theater	⠠⠠⠠⠠	three	⠠⠠⠠⠠
thumb	⠠⠠⠠⠠	week	⠠⠠⠠⠠	wrist	⠠⠠⠠⠠
<i>Animate Real Words</i>					
bird	⠠⠠⠠⠠	bull	⠠⠠⠠⠠	flea	⠠⠠⠠⠠
frog	⠠⠠⠠⠠	hawk	⠠⠠⠠⠠	lion	⠠⠠⠠⠠
mouse	⠠⠠⠠⠠	mule	⠠⠠⠠⠠	pony	⠠⠠⠠⠠
sheep*	⠠⠠⠠⠠	tiger	⠠⠠⠠⠠	trout	⠠⠠⠠⠠
whale	⠠⠠⠠⠠	wolf	⠠⠠⠠⠠	worm	⠠⠠⠠⠠
artist	⠠⠠⠠⠠	aunt	⠠⠠⠠⠠	clown	⠠⠠⠠⠠
cousin	⠠⠠⠠⠠	dancer	⠠⠠⠠⠠	farmer	⠠⠠⠠⠠
maid	⠠⠠⠠⠠	parent	⠠⠠⠠⠠	poet	⠠⠠⠠⠠
pope	⠠⠠⠠⠠	queen	⠠⠠⠠⠠	rabbi	⠠⠠⠠⠠
sister	⠠⠠⠠⠠	teacher	⠠⠠⠠⠠	wife	⠠⠠⠠⠠
<i>Pseudowords</i>					
broj	⠠⠠⠠⠠	cerov	⠠⠠⠠⠠	cheuq	⠠⠠⠠⠠
choner	⠠⠠⠠⠠	concak	⠠⠠⠠⠠	convuk	⠠⠠⠠⠠
coza	⠠⠠⠠⠠	eipar	⠠⠠⠠⠠	elni	⠠⠠⠠⠠
exedi	⠠⠠⠠⠠	fepin	⠠⠠⠠⠠	fihi	⠠⠠⠠⠠
fomp	⠠⠠⠠⠠	foreun	⠠⠠⠠⠠	grij	⠠⠠⠠⠠
haky	⠠⠠⠠⠠	hevero	⠠⠠⠠⠠	jaxin	⠠⠠⠠⠠
knab	⠠⠠⠠⠠	mirg	⠠⠠⠠⠠	opring	⠠⠠⠠⠠
sechu	⠠⠠⠠⠠	singpi	⠠⠠⠠⠠	susk	⠠⠠⠠⠠
swoud	⠠⠠⠠⠠	theanst	⠠⠠⠠⠠	thraz	⠠⠠⠠⠠
thuli	⠠⠠⠠⠠	weip	⠠⠠⠠⠠	wroz	⠠⠠⠠⠠

\* Our initial three participants saw “calf (⠠⠠⠠⠠)” rather than “sheep.” Because of the ambiguity of its meaning (a young cow, which is animate; a body part, which is inanimate), “calf” was replaced with “sheep” for the other participants.

reliable measurement per word. As a result, inanimate real words were the most frequent stimuli, each occurring 30 times throughout the experiment, whereas each

animate real word and each pseudoword was presented twice throughout the experiment. Our primary analyses thus focus on the inanimate words with secondary analyses looking at animate real words and pseudowords.

Each word/pseudoword was composed of exactly four braille cells and was presented in contracted braille. All stimuli in the current experiment were written in UEB, the most current braille system that all our participants were familiar with (Simpson, 2013). Although all words and pseudowords were exactly four braille cells long, they varied in uncontracted word length in Roman letter spelling from a minimum of four letters (e.g., “corn”) to a maximum of seven letters (e.g., “theater”). The length of individual inanimate real words in Roman letter spelling (i.e., the uncontracted form) was used as a predictor in fMRI modeling described below. We also examined the effect of the number of raised dots as a proxy for the amount of low-level somatosensory stimulation. Because uncontracted word length, our variable of interest, and dot-count are moderately correlated (Pearson  $r = .44$ ), these were included in the same fMRI model to separate their effects.

Uncontracted word length is highly correlated with the number of phonemes (Pearson  $r = .73$ ) and the number of syllables ( $r = .66$ ). Given the nature of English spelling, such correlations are nearly impossible to eliminate. Some theories of reading posit that phonological representations of words are retrieved during visual lexical decision, even when no phonological output is required (Leininger, 2014; Fiebach, Friederici, Müller, & von Cramon, 2002; Van Orden et al., 1988). Therefore, as discussed in detail below, we conducted control analyses to examine effects of phoneme number and syllable number on brain activity to better identify specifically orthographic length effects.

The experiment consisted of 15 runs (participants were free to take breaks between runs). In each run, all 30 inanimate real words were presented twice in different orders, and four distinct animate words and four distinct pseudowords were interspersed throughout the run in pseudo-random intervals. On average, there was one animate real word or pseudoword every seven inanimate words. Animate real words and pseudowords were never presented consecutively.

During the fMRI experiment, participants were instructed to read with the index finger of their preferred reading hand, and to press the response buttons using the other hand. Six of the 12 participants read with their right hands.

### fMRI Acquisition

All functional and structural MRI data were acquired at the F. M. Kirby Research Center of Functional Brain Imaging on a 3 T Phillips dStream Achieva scanner. T1-weighted structural images were collected in 150 axial slices with 1-mm isotropic voxels using a magnetization prepared rapid

gradient echo sequence. Functional T2\*-weighted BOLD scans were collected using a gradient EPI sequence with the following parameters: 36 sequential ascending axial slices, repetition time = 2 sec, echo time = 0.03 sec, flip angle = 70°, field of view matrix = 76 × 70, slice thickness = 2.5 mm, interslice gap = 0.5, slice-coverage feet-to-head = 107.5, voxel size = 2.53 × 2.47 × 2.50 mm, phase encoding direction = left to right, first order shimming. Six dummy scans were collected at the beginning of each run but were not saved.

## Analysis

### *Behavioral*

Behavioral analyses were performed in R (R Core Team, 2022). We used a linear mixed-effect ANOVA model implemented in the *nlme* package in R (Pinheiro, Bates, & R Core Team, 2022) to investigate the effect of word category (three categories: inanimate real word, animate real word, and pseudoword) on in-scanner response accuracy and RT. Because we collected multiple measurements for each word from each participant, in these behavioral analyses, participant and word were specified as crossed random effects (Baayen, Davidson, & Bates, 2008).

Linear mixed-effect multiple regression models were used to test for effects of uncontracted word length, the number of dots in each braille word (dot count), and word frequency (log transformed) on in-scanner response accuracy and RT, with participant and word specified as random effects. Because the fMRI analysis for word length and frequency concentrated on inanimate words (because of much larger data quantity for these words), we also focused behavioral analyses looking at effects of length and frequency on inanimate real words for consistency.

In addition, separate linear mixed-effect multiple regression analyses were conducted to examine the effect of phoneme count on accuracy and RT, controlling for log frequency. Another set of linear mixed-effect multiple regression were conducted to test the effect of syllable count, controlling for log frequency.

The R scripts used for these behavioral analyses are posted on our Open Science Framework repository: <https://osf.io/tnbd5/>.

### *fMRI Preprocessing and Analysis*

We used FMRIB Software Library, Freesurfer, the Human Connectome Project workbench, and in-house software to conduct preprocessing and univariate analyses. Functional data were motion-corrected, high-pass filtered with a 128-sec cutoff, and resampled to the cortical surface for each participant using the standard Freesurfer pipeline (Glasser et al., 2013; Smith et al., 2004; Dale, Fischl, & Sereno, 1999). The surface data were then smoothed with a 6-mm FWHM Gaussian kernel and prewhitened to remove temporal autocorrelation. Note that smoothing was

performed on the surface, rather than in the volume, and 6-mm smoothing on the surface corresponds to approximate 3-mm smoothing in the volume (Hagler, Saygin, & Sereno, 2006). Cerebellar and subcortical structures were excluded. Participant motion was low, despite the length of the experiment. On average, each participant had 0.42 time points in total with frame displacement root-mean-squared > 1.5 mm (across participant range min 0 to max 2,  $SD = 0.79$ ).

In each of the individual subject general linear models (GLMs) described below, we included a separate regressor to model out time points with excessive motion, defined as time points in which frame displacement root mean squared were greater than 1.5 mm (Kim et al., 2017). White matter signal and cerebral spinal fluid signal were also included in each of the individual subject GLMs as nuisance regressors.

In the individual subject GLMs, all predictors modeled only the first 3 sec of each trial during which a braille word was presented and were convolved with a canonical double-gamma hemodynamic response function (Smith et al., 2004). Within participants, data from different runs were combined using fixed effects models. Across participants, data were combined using a random-effects model. The resulting maps of  $p$  values underwent cluster-based non-parametric permutation correction to control the family-wise error rate (FWER) at  $p < .05$ , with cluster-forming threshold  $p < .01$  (Winkler, Ridgway, Webster, Smith, & Nichols, 2014; Nichols & Holmes, 2002). We chose non-parametric permutation correction because prior simulation and empirical work has shown that it controls FWER at the nominal level of 5% using this cluster-forming threshold and FWER (Eklund, Knutsson, & Nichols, 2019; Eklund, Nichols, & Knutsson, 2016; Winkler et al., 2014).

*Whole-cortex analysis of univariate uncontracted word length, dot number, and word frequency effects.* We modeled the effect of uncontracted word length for the inanimate real words (i.e., number of individual Roman letters in the spelling of each word), together with number of raised dots per word, as well as the logarithm of word frequency in the Corpus of Contemporary American English database (Davies, 2008). These predictors were included in a single univariate GLM. This analysis, which was intended to measure the effects of these three variables on real word processing, focused on inanimate words because each inanimate word was presented 30 times during the course of the experiment, compared with only twice for animate and pseudowords, providing a much better measure of neural response.

All predictors were mean centered before entry into the GLM. The number of raised dots was moderately correlated with uncontracted word length ( $r = .44, p < .05$ ) and were thus included in the same GLM to test for the unique statistical contribution of each variable to neural activity, controlling for the other. Word frequency (log-transformed) was not significantly correlated with

uncontracted word length ( $r = -.31, p = .1$ ) and were also included in the same fMRI model to study their independent effects.

Because uncontracted word length (letter count) is inevitably highly correlated with phoneme and syllable count (in the current sample letters vs. phonemes:  $r = .73$ ; letters vs. syllables:  $r = .66$ ), we additionally ran control GLMs testing separately for phoneme and syllable count effects on neural activity. Neither phoneme nor syllable length significantly predicted neural activity anywhere on the cortical surface. Note, however, that because uncontracted word length, phoneme count, and syllable count are highly correlated, we did not enter these into the same GLM model and therefore cannot unambiguously separate their effects. The conclusion that phoneme or syllable count do not affect brain activity is therefore based on the null effects of these variables.

In these analyses, length and frequency predictors were used to calculate the within-subject beta values that served as input to nonparametric random-effects subject-wise analyses that do not assume normality (Winkler et al., 2014; Nichols & Holmes, 2002).

In all the GLMs testing for uncontracted word-length effects described above, besides the predictors for length, dot-number, and frequency, four other predictors were included in the model to control for the effects of word category (inanimate real word, animate real word, and pseudoword) and missed trials. Missed trials were those which participants failed to respond. They were excluded because we could not verify that participants had read the word and attempted to do the task. Incorrect responses (which only constituted 1.9% of all 12,240 trials administered across all participants) were included because some animacy judgments are ambiguous (e.g., body parts) and we were primarily interested in whether the participant had read the word, not in the decision they made.

To test whether the lateralization of uncontracted word length effect and the dot count effect were driven by reading hand, we compared the laterality index between left-hand readers ( $n = 6$ ) and right-hand readers ( $n = 6$ ). Laterality index is defined as  $(L - R) / (L + R)$ , where L and R are the sums of the  $z$ -statistics for the relevant effect in the left and the right hemispheres, respectively. For the uncontracted word length effect, we considered the  $z$ -statistics within a supramarginal gyrus (SMG) ROI, which was the union of the vertices on both hemispheres revealed by the group contrast of the uncontracted word length effect. For the dot count effect, we used the hand region of the left primary somatosensory cortex (S1) from Neurosynth. The resultant laterality indices were Fisher- $z$  transformed before being submitted to an independent-samples  $t$  test to compare between left- and right-hand readers.

*Whole-cortex univariate words versus pseudoword comparison.* In this univariate GLM analysis, for each vertex on the cortical surface, three predictors modeled

the effect of inanimate real words, animate real words, and pseudowords, respectively. A separate predictor was added to model missed trials. Because behavioral analysis revealed a significant difference in RT among the three word categories, we included a fifth predictor to model the effect of RT (Yarkoni, Barch, Gray, Conturo, & Braver, 2009). The main results report the contrast between inanimate real words and pseudowords, because we have more data for inanimate words and therefore more reliable measures. Results comparing animate real words to pseudowords were consistent with results from the inanimate word contrast but weaker.

### MVPA

*Support vector machine decoding of real words versus pseudowords.* Support vector machine (SVM) decoding implemented in the Python toolbox Scikit-learn was used to distinguish real words from pseudowords based on the spatial activation pattern (Chang & Lin, 2011; Pedregosa et al., 2011; Kriegeskorte, Goebel, & Bandettini, 2006). A GLM was constructed in which each animate, inanimate, and pseudoword was entered as an individual predictor, along with a predictor for missed trials and another predictor for RT for each stimulus word. The resultant betas were then normalized. The real word and pseudoword data were separately normalized across items and vertices to ensure that decoding was based on the difference in spatial pattern rather than univariate activation level. Normalization was done by subtracting the mean value and dividing by the standard deviation across patterns and vertices (Mahmoudi, Takerkart, Regragui, Boussaoud, & Brovelli, 2012; Misaki, Kim, Bandettini, & Kriegeskorte, 2010). The normalized beta maps were entered as the training/testing data for the decoding analysis, after normalization.

Whole-cortex searchlight analyses were performed on the inflated cortical surface, with each searchlight consisted of all the vertices within a circle of 8-mm diameter (according to geodesic distance) centered at the vertex (Glasser et al., 2013; Kriegeskorte et al., 2006). Vertices whose corresponding searchlight contained any subcortical vertex were excluded.

We used a permutation and bootstrapping-based method to test the classifier performance against chance (50%; Elli, Lane, & Bedny, 2019; Schreiber & Kregelberg, 2013; Stelzer, Chen, & Turner, 2013). For each participant, at each vertex, the accuracy value was Fisher- $z$  transformed. We then computed the  $t$  statistics of the group mean (across participants) when tested against chance (which was also Fisher- $z$  transformed). This step resulted in a map of  $t$  statistics. For each participant, we shuffled the word labels (“inanimate word” and “pseudoword”) 200 times and derived one null accuracy map per shuffle. For each shuffle, we similarly derived across participants a map of  $t$  statistics. Next, in each vertex, we defined the empirical  $p$  value as the probability of observing, in the

normal distribution formed by the null values, a  $t$  statistic higher than the actual  $t$  value.

The resulting maps of  $p$  values underwent cluster-based permutation correction to control the FWER (Su, Fonteneau, Marslen-Wilson, & Kriegeskorte, 2012). The cluster-forming threshold was uncorrected  $p < .01$ , and the cluster-wise FWER threshold was  $p < .05$ . Permutation correction has been shown to adequately control FWER at the nominal level of 5% using this cluster-forming and FWER (Eklund et al., 2016, 2019; Winkler et al., 2014).

The main decoding analysis focused on distinguishing real inanimate words from pseudowords, because we had by far a larger amount of data for the inanimate than animate real words and therefore a more reliable measure. We also performed a comparable whole-cortex searchlight SVM decoding analysis to distinguish between real animate words and pseudowords. The results of this analysis were consistent with the inanimate real word versus pseudoword analysis but weaker.

Because each inanimate real word appeared 30 times (twice per run), but each pseudoword appeared only twice throughout the experiment, we took several steps to ensure that decoding of inanimate words versus pseudowords was not driven by different degrees of noise across conditions. First, we matched the number of trials that contributed to the beta estimate of each word/pseudoword across conditions by extracting one beta parameter estimate per run for each inanimate real word, for each participant, and extracting one pseudoword beta for each participant, across runs. This resulted in the same number of trials (two for each entry) contributing to the estimates of betas for each entry of words and pseudowords. Consequently, in the training data set for each participant, there was one spatial pattern of beta estimates for each pseudoword and 15 patterns for each inanimate real word (one pattern from each run). Next, we matched the number of training patterns across conditions by splitting the real inanimate word beta patterns (total of 450) into 15 decoding bins. In each decoding bin, each run contributed the beta patterns of two and only two words. The words contributed by the runs were rotated through bins. Suppose in Bin 1, the beta patterns of the words “bread” and “honey” come from Run 1, and the beta patterns of the words “cereal” and “milk” come from Run 15. Then, in Bin 2, “bread” and “honey” are derived from Run 2, whereas “cereal” and “milk” are from Run 1.

Each of the 15 classifiers was trained to distinguish words and pseudowords using only one of the 15 beta estimate patterns from each inanimate word, each pattern derived from two trials, and likewise one pattern for each pseudoword, also derived from two trials of that pseudoword. Thus, each classifier had an equivalent amount of data for real and pseudowords. In each of the 15 decoding bins, in each searchlight region, we trained a linear SVM classifier (regularization parameter  $C = 1$ ) on 90% of the

data (27 inanimate words and 27 pseudowords) and tested it on the left out 10% of the data. The decoding accuracy was averaged across 10 train-test splits to derive the accuracy for each decoding bin. Then, the accuracy was averaged across all 15 bins to derive the accuracy for the center vertex of a given searchlight region. Eventually, this analysis yielded one whole-brain classification accuracy map for each participant.

### *Neural Signatures of Individual Braille Words: Split-half MVPA Correlation Analysis*

In a final analysis, we used MVPA to search for neural signatures of individual braille words. Specifically, we conducted a split-half correlation analysis to investigate whether any cortical areas showed unique spatial patterns of response to specific inanimate real braille words that were distinguishable from all other inanimate braille words in our stimulus set.

In the split-half correlation analysis, we split the data from 15 runs into even runs and odd runs with Run 7 excluded so that both halves contained the same number of runs. We computed one fixed effect beta parameter estimation map for each of the 30 words in each half, based on which we created a  $30 \times 30$  similarity matrix between the words in each searchlight. For a diagonal entry ( $i, i$ ) in such matrix, we computed the Pearson correlation between the spatial pattern of word  $i$  in the even half and the pattern of word  $i$  in the odd half. For an off-diagonal entry ( $i, j$ ) in such matrix, we computed the correlation between word  $i$  in the even half and word  $j$  in the odd half, and the correlation between word  $j$  in the even half and word  $i$  in the odd half, and then took the average of the two correlation values. In each participant, if each word is consistently represented in a searchlight, the spatial patterns of the same word from both halves should be highly correlated, whereas the patterns of different words should be uncorrelated, leading to the values in the diagonal of the similarity matrix close to 1 and the off-diagonal entries close to 0. We used a bootstrapping method to test this hypothesis. In each searchlight, we computed the mean value across the diagonal entries of the similarity matrix, denoted as  $M$ . Then, we computed the mean and standard deviation of the off-diagonal entries in the upper triangle. Next, we computed the  $z$  score of  $M$  with respect to the distribution of the off-diagonal values (assuming the off-diagonal values were normally distributed). To test the statistical significance of the resultant  $z$ -score in each searchlight, we shuffled all the values in the upper triangle and diagonal entries to create a null similarity matrix and repeated the previous steps to derive a null  $z$  scores. The similarity matrix was shuffled 200 times to derive a null distribution of the  $z$  scores based on which the  $p$  values of the observed  $z$  score was derived. The average  $z$  score map across participants underwent FWER correction with a cluster-forming threshold of uncorrected  $p < .01$  and cluster-wise  $p < .05$ .

As a separate attempt in search for the signature of individual inanimate real words, we conducted a whole-cortex searchlight 30-way SVM decoding analysis, and an ROI-based 30-way SVM decoding (with ROIs defined by the inanimate-versus-pseudocode two-way decoding results). However, neither the whole cortex nor the ROI-based SVM decoding analyses yielded any significant results and we therefore do not discuss them further here.

## RESULTS

### Behavioral

Participants were highly accurate across conditions, with the highest accuracy for inanimate real words ( $M = 98.8\%$ ,  $SD = 2.8\%$ ), followed by pseudowords ( $M = 93.8\%$ ,  $SD = 4.6\%$ ), and finally by animate real words ( $M = 91.1\%$ ,  $SD = 11.5\%$ ; effect of word category; real inanimate, real animate, and pseudo) in mixed-effect ANOVA,  $F(2, 1066) = 25.9$ ,  $p < .001$ . Post hoc comparisons showed that the difference between inanimate real word and pseudoword was significant,  $t(1066) = 4.68$ ,  $p < .001$ , so was the difference between pseudoword and animate word,  $t(1066) = 2.01$ ,  $p < .05$ . The high accuracy suggests that despite the length of the experiment, participants remained attentive throughout (Figure A1).

Participants responded the fastest to inanimate real words ( $M = 1.02$  sec,  $SD = 0.38$  sec), followed by animate real words ( $M = 1.55$  sec,  $SD = 0.49$  sec), and slowest to pseudowords ( $M = 1.90$  sec,  $SD = 0.69$  sec; mixed-effect ANOVA,  $F(2, 1066) = 971.02$ ,  $p < .001$ ). Post hoc comparisons showed the response to inanimate real words was significantly faster than to animate real words,  $t(1066) = -26.29$ ,  $p < .001$ , and the response to animate real words was, in turn, significantly faster than to pseudowords,  $t(1066) = -9.91$ ,  $p < .001$  (Figure A1).

In a mixed-effect multiple regression model including uncontracted word length, dot count, and log-transformed word frequency, there was no effect of uncontracted word length on accuracy ( $\beta = -0.004$ ,  $SE = 0.004$ ,  $p = .31$ ) or RT ( $\beta = -0.005$ ,  $SE = 0.009$ ,  $p = .60$ ). In other words, contracted words whose corresponding uncontracted forms have more letters did not take more time to read than uncontracted words with the same number of cells, nor did they lead to more errors in the lexicality judgment in the current experiment. Responses to words with more dots were more accurate ( $\beta = 0.005$ ,  $SE = 0.002$ ,  $p < .05$ ) but not different in RT ( $\beta = 0.01$ ,  $SE = 0.005$ ,  $p = .07$ ). Words with higher frequency were responded to with marginally higher accuracy ( $\beta = 0.012$ ,  $SE = 0.006$ ,  $p = .05$ ), and the RT for higher frequency words was significantly shorter than for lower frequency ones ( $\beta = -0.041$ ,  $SE = 0.013$ ,  $p < .01$ ).

As for number of phonemes and number of syllables, the two variables highly correlated with uncontracted

word length, in separate mixed-effect multiple regression models, we found no effect of either variable on either accuracy or RT ( $ps > .05$ ).

### fMRI

#### *Neural Activity Increases in Bilateral PPC with Uncontracted Word Length: Univariate Whole-cortex Analysis*

In a whole-cortex analysis, we searched for cortical areas where activity increased as the uncontracted forms of words became longer in number of Roman letters, independent of physical word length in braille cells (all words had the same number of braille cells). Bilateral PPC, specifically the SMG (peak: left  $-36$ ,  $-35$ ,  $37$ ; right  $57$ ,  $-33$ ,  $48$ ), responded more to words with a greater uncontracted word length (Figure 1). No regions increased activity as the corresponding uncontracted words became shorter.

To investigate whether laterality of observed effects was driven by reading hand, we compared the laterality index of the uncontracted word length effect between the left- ( $n = 6$ ) and the right-hand ( $n = 6$ ) readers. We found no difference in laterality between the groups (left-handers mean =  $-0.11$ , right-handers mean =  $-0.20$ ,  $t(5) = 0.50$ ,  $p = .63$ ). This suggests that bilateral SMG responses result from a bilateral effect in each participant. Note that such null lateralization results should be interpreted with caution because the current study is not powered to detect individual differences.

For the words used in this experiment, another variable that was moderately, but significantly, correlated with uncontracted word length was the number of raised dots in a word, because the cells corresponding to contractions are, on average, more likely to have a larger number of dots than those corresponding to individual letters. For the 30 inanimate real words used in this experiment, the correlation between uncontracted word length and dot count is  $r = .44$ . In the same analysis that evaluated the effect of uncontracted word length effect, we included the number of dots as a separate predictor. We observed an increase in activity as a function of dot count in the hand region of the left primary somatosensory cortex (S1). Figure 1 shows this activation relative to an outline of the hand region for left sensorimotor cortex from Neurosynth (Tian et al., 2022; Loiotile, Lane, Omaki, & Bedny, 2020). This effect was clearly superior and anterior and disjoint from the cluster showing the uncontracted word length effect. A dot-number effect was also observed in the right STS.

Similar to the uncontracted word length effect, we compared the laterality index of the dot count effect between left- and right-handed readers. We found no difference between the groups (left-handers mean =  $0.16$ , right-handers mean =  $0.35$ ,  $t(5) = -0.77$ ,  $p = .46$ ).

We conducted two additional whole-cortex univariate analyses where the predictor for uncontracted word

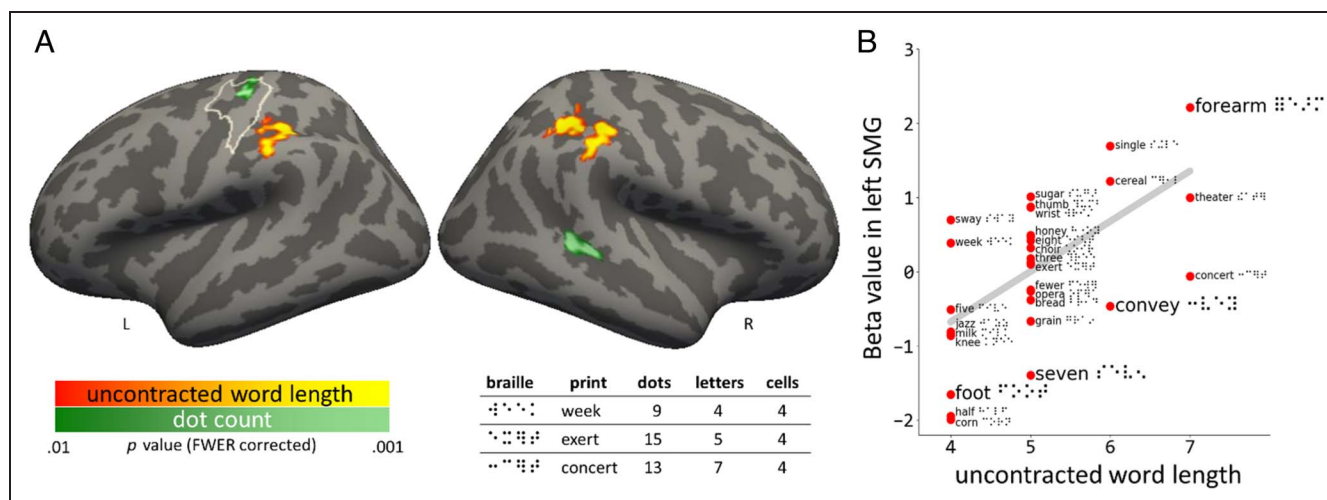


**Figure 1.** (A) Red/yellow: regions showing greater response to four-cell Braille words that contain more letters when transcribed to written English. Dark/bright green: regions showing greater response to 4-cell Braille words that contain more raised dots. The brain map was cluster-based permutation corrected to control the FWER. The cluster-forming threshold was uncorrected  $p < .01$ , and the cluster-wise FWER threshold was  $p < .05$ . Bottom right: examples of Braille words in this experiment with the least dots (week) and the most dots (exert); “week” is also one of the shortest words in Roman spelling (four letters), whereas “concert” is one of the longest (seven letters). White outlines mark the hand S1/M1 region. (B) The correlation between word length in uncontracted Roman spelling and neural activation in the left supramarginal gyri (SMG), measured with the beta estimation for the activation level of each word. For illustration purpose, in the left SMG, for each word, we averaged the beta value across the vertices and across participants. Then, we correlated the average beta values with the word lengths.

length was replaced by a predictor for number of phonemes and number of syllables, respectively. Despite the high correlation between the numbers of letters, phonemes, and syllables (letters vs. phonemes:  $r = .73$ ; letters vs. syllables:  $r = .66$ ), we did not find an effect of the number of phonemes or syllables under the same threshold and statistical correction as used for number of letters. Nevertheless, because of the high correlation between the numbers of letters and phonemes in English, we cannot unambiguously distinguish between an orthographic effect of underlying uncontracted word length (number of letters) and a phonological effect of the underlying numbers of phonemes or syllables.

#### *Neural Effects of Word Frequency Are Differently Localized from Effects of Uncontracted Word Length: Univariate Whole-cortex Analysis*

In the same analysis in which we investigated the effect of uncontracted word length and number of raised dots, we also included word frequency (log transformed) as a separate predictor. The analysis results showed sensitivity to word frequency was localized to different cortical areas from those that exhibited sensitivity to uncontracted word length (above). We observed significantly larger responses to low frequency words in the left inferior frontal sulcus (IFS), left superior frontal gyrus, right fusiform gyrus, and right anterior inferior/middle temporal gyri. No regions were significantly more responsive to higher compared with lower frequency words. No word frequency effects were observed in the SMG or anywhere in the PPC (Figure A2).

#### *Univariate Differences between Words versus Pseudowords in Whole-cortex Analysis*

We observed larger responses to pseudowords than words (inanimate) bilaterally in the PPC (intraparietal sulcus [IPS] and SMG) and in the inferior frontal cortex (IFS/precentral sulcus [PCS], anterior insula; Figure 2A). Larger responses to pseudowords than words were also observed in ventral occipito-temporal cortex vOTC (fusiform gyrus) bilaterally. vOTC responses were located medial and anterior to the location of the VWFA region as defined based on a meta-analysis carried out by Jobard and colleagues (2003). Some responses were also observed lateral to this VWFA location, extending into the inferior temporal gyrus and the middle occipital sulcus on the lateral surface. Larger responses to pseudowords were also observed in dorsal occipital and parieto-occipital areas as well as in right primary visual cortex. We observed a qualitatively similar but weaker effects when comparing pseudowords to animate real words.

Interestingly, the parietal regions showing sensitivity to uncontracted word length overlapped with the parietal regions that were more active for pseudowords relative to real inanimate words (Figure 2; see Figure 3 for the overlap), despite the fact that pseudowords were not included in the uncontracted word length analysis. This provides further evidence for the possibility that these parietal regions play a role in form-based orthographic braille processing, perhaps the conversion from contracted to uncontracted Roman spellings and/or from graphemes to phonemes.

The univariate contrast of words (inanimate) versus pseudowords revealed greater activation for words in

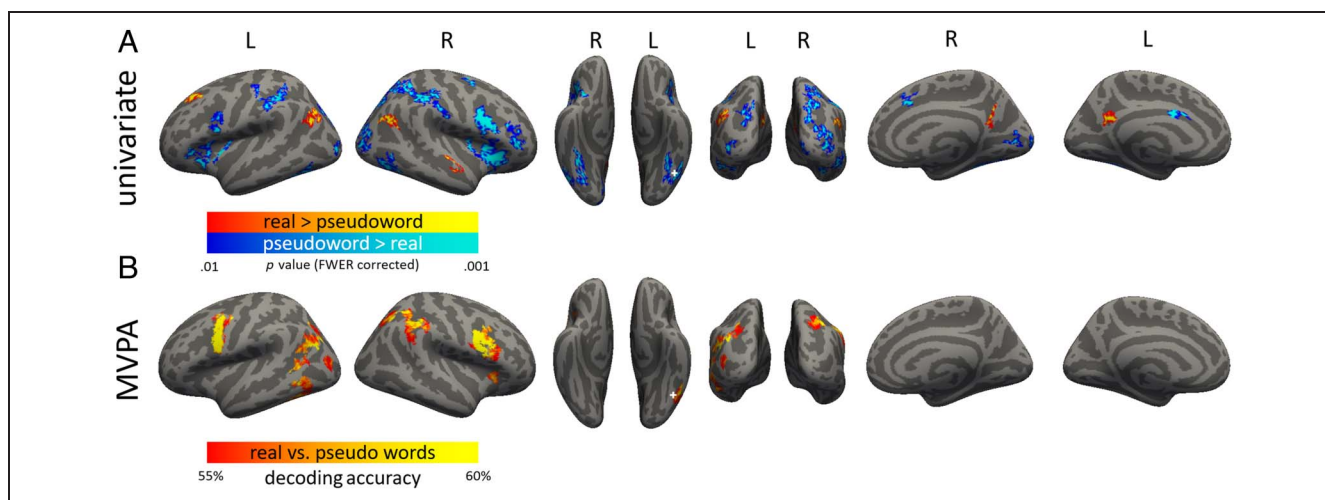


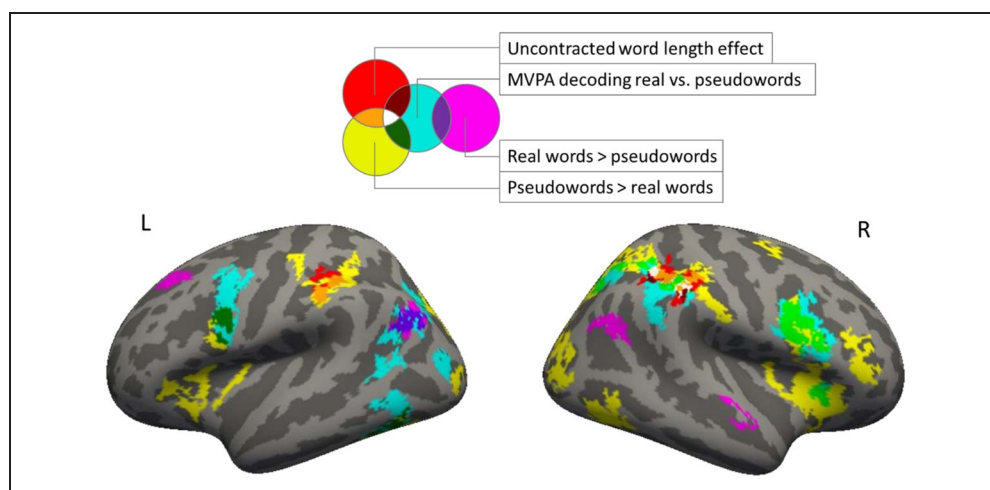
**Figure 2.** Differences in the neural response to real words and pseudowords. (A) univariate contrasts. Warm color: real words > pseudowords. Cool color: pseudowords > real words. (B) Real word versus pseudoword MVPA decoding accuracy. Chance level of decoding accuracy = 50%. Both maps underwent cluster-based permutation correction to control the FWER. The cluster-forming threshold was uncorrected  $p < .01$ , and the cluster-wise FWER threshold was  $p < .05$ . The peak of the VWFA reported by Jobard and colleagues (2003) is marked with the white cross. “Real word” refers to inanimate real words. Please see the main text for details.

areas associated with semantic processing, including the bilateral precuneus (PC) and on the lateral surface bilateral temporo-parietal cortex (angular gyri [AG]; Figure 2A). Small clusters were also observed in the right anterior superior temporal gyrus and left superior frontal sulcus. A comparison between animate real words and pseudowords revealed effects consistent to those observed with inanimate words but weaker.

Finally, because participants pressed different buttons (for different numbers of trials) for real inanimate, real animate, and pseudowords, a potential worry is that differences between pseudo and inanimate words observed in parietal cortex could be related to different motor responses, different task-related decisions, or different frequency of responses across these inanimate words and pseudowords. Because participants also made different

responses and different numbers of responses to inanimate and animate real words, we compared these conditions as a control. If decision characteristics/frequency of response is driving the parietal effects, we should observe the same differences between real animate and real inanimate words. The comparison between inanimate and animate real words suggests that parietal differences between real and pseudowords are unlikely to be driven solely by different response characteristics. Specifically, we did not observe activation difference between animate and inanimate words in the portions of parietal cortex that were especially responded to pseudowords or in the SMG, even under an uncorrected threshold. In addition, when we overlaid the contrasts “animate > inanimate real word” and “pseudoword > inanimate real word,” we did not see any overlap in bilateral SMG (Figure A3).

**Figure 3.** Overlap between four maps: univariate inanimate real words > pseudowords (R > P, magenta), univariate pseudowords > inanimate real words (P > R, yellow), MVPA decoding (MVPA, cyan), uncontracted word length effect (LEN, red). Purple: overlap between R > P and MVPA. Green: overlap between P > R and MVPA. Orange: overlap between P > R and LEN. Dark red: overlap between MVPA and LEN. White: overlap between P > R, MVPA, and LEN. Overlap between LEN and MVPA or P > R (orange, dark red, and white) indicates orthographic processing. Overlap between MVPA and R > P (purple) indicates semantic processing.



### Words versus Pseudowords MVPA Whole-cortex Analysis

Real words (inanimate) and pseudowords produced different MVPA patterns in right PPC (SMG, extending into the AG and the IPS) and inferior frontal cortex (in bilateral IFS/PCS and right anterior insula; Figure 2B). These areas overlapped with univariate pseudoword responses as well as to some extent with uncontracted word length responsive areas. There was also some overlap with responses to words in the left temporo-parietal junction (AG, extending ventrally into the posterior STS dorsally into the posterior IPS). Additional areas of significant decoding that did not overlap with the univariate analysis were observed in left occipital and occipito-temporal cortices (posterior inferior temporal sulcus and middle occipital sulcus/gyrus). The MVPA decoding for animate real words versus pseudowords yielded a similar spatial pattern of decoding accuracy to the inanimate words versus pseudowords comparison, but with lower accuracy values and no cluster surviving the permutation test correcting for FWER (Figure A4).

### Exploratory Analyses of Univariate and Multivariate Effects in the vOTC at a Lower Threshold

Given the involvement of VWFA in the processing of orthography in the sighted and prior reports of responses to braille in this region, we searched for effects in the vOTC at an exploratory threshold to see if effects in the classic VWFA location would emerge ( $p$  values less than .05, uncorrected). At this exploratory threshold, in the pseudowords > inanimate real words univariate contrast, activation differences were observed throughout the left vOTC, including but not limited to the VWFA location. In the map of significant MVPA decoding of pseudowords versus words and the map of significant sensitivity to uncontracted word length effect, even at this exploratory threshold, the involvement of the left vOTC was restricted to the inferior temporal sulcus and anterior fusiform gyrus. In the map depicting the negative frequency effect (higher activation for lower frequency words), the lateral and medial portion of the left vOTC were identified, but in both maps, the peak of the VWFA as reported in the meta-analysis by Jobard and colleagues (2003) was not recruited (Figure A5).

### Neural Signatures of Individual Braille Words: Split-half MVPA Correlation Analysis

We attempted to identify cortical areas containing information about individual word identities, relative to all other words in our stimulus set. In a whole-cortex searchlight split-half analysis that searched for cortical regions where the similarity between a word and itself was greater than between that word and all other words in the stimulus set, we observed small significant clusters in bilateral inferior PCS, bilateral posterior IPS, bilateral PC, and

left posterior STS. Except for the clusters in bilateral PC, these clusters overlapped with the regions that distinguished between inanimate words and pseudowords in the whole-cortex searchlight SVM decoding analysis (Figure A6).

## DISCUSSION

We observed orthographic reading-related effects for braille that were separable from low-level tactile and high-level semantic processes in the PPCs. Activation in bilateral SMG (left  $-36, -36, 37$ ; right  $33, -44, 40$ ) was positively correlated with the word length of uncontracted spelling corresponding to the contracted braille words that the participants were actually reading. Specifically, braille words consisting of the same number of cells but with more letters in their corresponding uncontracted forms (e.g., “milk,” ⠠⠍⠢⠎⠇ vs. “concert” ⠠⠎⠠⠗⠠⠗⠠) produced higher SMG activity. Neither the number of syllables, phonemes, or braille dots predicted this SMG effect, suggesting a specific role in tactile orthographic processing for the SMG. By contrast, the hand region of primary somatosensory cortex was sensitive to total dot number per word, a proxy for the amount of somatosensory stimulation. In the current study and in prior work, contractions did not slow down proficient readers (Millar, 1997). Thus, rather than reflecting reading difficulty, the effect of the uncontracted word length is likely to reflect the retrieval of the sublexical units in braille (Fischer-Baum & Englebretson, 2016). One possibility is that, in addition to understanding contractions as stand-alone symbols, letters represented by the contractions are retrieved and reorganized according to the morphological structure of the word (Fischer-Baum & Englebretson, 2016).

In addition to showing an uncontracted word length effect, bilateral SMG also showed greater activation for pseudowords than real words and right SMG showed above-chance MVPA decoding of real and pseudowords, although the pseudowords did not differ from real words in low-level tactile properties. An extensive literature on visual reading has identified different neural responses to pseudo and real words (Choi, Desai, & Henderson, 2014; Taylor et al., 2013; Heim et al., 2005; Ischebeck et al., 2004; Mechelli et al., 2003; Price et al., 1996). To our knowledge, only one previous fMRI study has compared real Braille word to pseudo-word reading, and that study used only univariate methods (Dzięgiel-Fivet et al., 2021). That study did not report any difference between real and pseudowords. It is not clear why we observed effects where none were found in that previous experiment. One possible difference is that the previous study involved passive reading, whereas we used an active lexical decision and semantic dual task, which explicitly required participants to attend to the lexico-semantic contents of individual words. It is possible that in-depth processing is required for real/pseudoword differences to be observed in braille and the current tasks encouraged such

processing. It is also possible that the explicit task of deciding whether a word was real or pseudo, and even the corresponding motor response, contributed to the observed effect. In control analyses, we show that the “animate > inanimate real word” contrast yields different results from the “pseudoword > inanimate real word” contrast, suggesting that mere differences in motor responses do not explain condition effects. Future work will determine whether the pseudoword effects observed in the current study generalize to other tasks, including more naturalistic oral and covert text reading, in which participants read sentences and even stories without explicitly deciding on the lexico-semantic properties of individual words.

Another limitation in interpreting the observed pseudoword effect is the imbalanced numbers of trials across some of the word and pseudoword conditions (each participant was presented with 900 inanimate real word trials, 60 animate real word trials, and 60 pseudoword trials). We attempted to control for this imbalance analytically. In the MVPA analysis comparing inanimate real and pseudowords, we made sure that each sample in the training data was derived from the same number of trials, and the classifier was given the same amount of training data from both conditions. We also observed largely similar real versus pseudoword effects when comparing conditions matched on number of trials: animate word versus pseudoword conditions. Nevertheless, future studies will be needed to verify the neural difference between real words and pseudowords when the number of real and pseudowords is matched.

In the whole-cortex analyses, only the right SMG exhibited all three effects: the uncontracted word length effect, the pseudoword preference, and differentiation of real versus pseudowords in MVPA. These results suggest that the SMG is involved in the retrieval of uncontracted spellings. The convergence of all three effects in SMG also serves as strong evidence for the specialization for Braille orthography in this region. In contrast, the right dorsal occipito-parietal and bilateral prefrontal cortices also distinguished pseudowords from real words but did not show an uncontracted word length effect. One interpretation of this result is that these regions are also involved in the orthographic processing of Braille but not specifically in the retrieval of uncontracted spellings. Alternatively, these areas may not be specialized for orthographic processing per se but may perform more general lexical retrieval functions. These alternatives can be distinguished in future studies of braille reading using different tasks and stimuli.

An intriguing possibility is that the PPC becomes recruited for braille orthography because of its role in high-level tactile texture and shape perception, analogous to the vOTC’s role in visual object recognition (Chivukula et al., 2021; Debowska et al., 2016; Sathian, 2016; Stilla, Deshpande, LaConte, Hu, & Sathian, 2007; Ro, Wallace, Hagedorn, Farne, & Pienkos, 2004; Burton, MacLeod,

Videen, & Raichle, 1997). The SMG is involved in tactile pattern perception and active touch (Li Hegner, Lee, Grodd, & Braun, 2010; Bodegård, Geyer, Grefkes, Zilles, & Roland, 2001). Damage to the PPC can cause tactile agnosia: the inability to recognize or name shapes from touch, in the absence of low-level somatosensory deficits (Veronelli, Ginex, Dinacci, Cappa, & Corbo, 2014; Bohlhalter, Fretz, & Weder, 2002). After sighted individuals received braille training for 3 weeks, structural and functional changes are found in the PPC, in addition to the primary somatosensory cortex (Debowska et al., 2016). The PPC is also structurally connected to somatosensory and language networks (Mohan, de Haan, Mansvelder, & de Kock, 2018; Burks et al., 2017; Margulies & Petrides, 2013; Save & Poucet, 2009; Frey, Campbell, Pike, & Petrides, 2008; Catani, Jones, & Ffytche, 2005; Parker et al., 2005). This body of evidence leads to the hypothesis that the PPC may play a role in braille word recognition analogous to that of the VWFA in visual word recognition, a hypothesis that is supported by our current findings.

Another possibility is that the PPC contributes to braille reading by performing grapheme-to-phoneme conversion, analogous to what has sometimes been proposed in sighted reading (Church, Balota, Petersen, & Schlaggar, 2011; Graves et al., 2010; Stoeckel, Gough, Watkins, & Devlin, 2009; Jobard et al., 2003). However, our findings that the activation in the PPC was not proportional to the number of phonemes or syllables disfavor this possibility. Yet another possible function instantiated in the PPC is orthographic working memory (sometimes referred to as the “graphemic buffer”), which supports the maintenance of the letters in a word in their precise order during reading and spelling (Purcell, Rapp, & Martin, 2021; Tainturier & Rapp, 2003; Caramazza, Capasso, & Miceli, 1996). The orthographic working memory system has been shown to be specifically taxed when the letters are accessed sequentially and/or in an attentionally demanding fashion. Past studies with sighted visual readers engaged this system or in visual tasks by making the words harder to read, by presenting one letter at a time, or by asking participants to spell words (Carreiras, Quiñones, Hernández-Cabrera, & Duñabeitia, 2015; Purcell et al., 2011; Rapp & Dufor, 2011; Cohen et al., 2008). Because we found that the activation in the PPC is proportional to the uncontracted word length, one possibility is that it maintains the letters in uncontracted spelling. However, the maintenance of such letters is not mutually exclusive with the function of letter retrieval and identification. Although the PPC may be specialized for either of these functions, it may also instantiate both of them. In future studies, we may seek to disentangle these possibilities.

In addition to effects in parietal and prefrontal cortices, we also observed univariate and MVPA sensitivity to pseudowords in the vOTC and the lateral inferior temporal gyrus, consistent with the idea that parts of the ventral stream play a role in braille processing. However, unlike

previous studies that contrasted braille against lower-level control conditions in blind readers, the vOTC effects we observed did not show a clear focal peak at the canonical anatomical location associated with the VWFA ( $-42, -57, -15$ ; Chen et al., 2019; Vogel et al., 2012; Kronbichler et al., 2004; Cohen et al., 2002). Instead, we observed responses both medial and lateral to the typical VWFA location. Medial parts of the vOTC are connected with parietal circuits, including the SMG, as well as dorsal occipital cortex (Jitsuishi et al., 2020; Bouhali et al., 2019; Moulton et al., 2019; Leo et al., 2012). This connectivity could convey orthographic information to the vOTC. On the other hand, the VWFA location itself may be the peak of linguistic rather than orthographic responses during braille reading. Such linguistic processes, (1) are not specific to written orthography but also relevant for spoken language and (2) include not only single-word retrieval, but also high-level processes such as syntax parsing and construction of compositional semantics. In sighted individuals, these high-level and amodal linguistic processes have been associated with the fronto-temporal language system (Fedorenko et al., 2016; Fedorenko & Varley, 2016; Blank, Kanwisher, & Fedorenko, 2014; Friederici & Gierhan, 2013; Friederici, Rueschemeyer, Hahne, & Fiebach, 2003). However, in congenitally blind, but not in sighted, individuals, the vOTC has been shown sensitive to high-level linguistic properties such as syntax complexity and the meanings of words (Tian et al., 2022; Lane, Kanjlia, Omaki, & Bedny, 2015; Bedny, Pascual-Leone, Dodell-Feder, Fedorenko, & Saxe, 2011). Consistent with this possibility, Dzięgiel-Fivet and colleagues (2021) recently reported speech-to-reading convergence in the vOTC of blind but not sighted participants, also suggesting that the vOTC may be involved in amodal linguistic processing for blind readers. Consistent with the idea that in people born blind, the vOTC may be involved in amodal language processes, rather than or in addition to reading-specific processes, the current study did not find evidence for orthographic specialization in the vOTC. Rather, orthographic effects were more robustly observed in the SMG.

Notably, most of the orthographic responses observed in the current study were bilateral and, if anything, somewhat stronger in the right hemisphere. The uncontracted word length effect in SMG was larger on the right, and parietal responses to nonwords were also right-lateralized. This is different from the left-lateralized responses to orthography generally observed during visual print reading by sighted people. Right-lateralized responses to orthography in blindness could be related to changes in spoken language lateralization in people born blind. Previous studies have found that spoken language is less consistently left-lateralized among blind than sighted people (Lane et al., 2017; Röder, Stock, Bien, Neville, & Rösler, 2002). One previous study also found that the lateralization of responses to braille are correlated with the laterality

of spoken language across blind individuals (Tian et al., 2022). Those blind individuals with right-lateralized responses to speech are also more likely to have right-lateralized responses to braille, particularly at higher stages of processing. Another variable that influences braille lateralization is reading hand. A previous study with a larger sample of participants reported that, in posterior parietal cortex, the laterality of braille reading (word reading > rest) was predicted jointly by reading hand and spoken language lateralization (Tian et al., 2022). In the current study, we did not find a relationship between reading-hand and the lateralization of the uncontracted word length effect. Participants who used their left or right hand to read were equally likely to exhibit a left- or right-lateralized uncontracted word length effect. One possibility is that the retrieval of the uncontracted spelling of braille words is at a higher level of processing than generalized responsiveness to braille words measured by Tian and colleagues (2022), and thus not tethered to the reading-hand hemisphere in the same way. However, given the small number of participants (six left-handers and six right-handers), the current study is not powered for an individual difference analyses and the absence of a significant reading hand effect should be interpreted with caution. Future studies should systematically investigate the laterality of the uncontracted word length effect and its relationship to reading hand and spoken language lateralization.

Finally, we were able to decode individual braille words based on patterns of activity in prefrontal, parieto-occipital, and occipito-temporal areas. Notably, these effects fell outside of S1, suggesting the decoding was based on something other than low-level sensory properties. This is unsurprising because previous studies of S1 have only decoded responses to tactile stimulation of different positions along the length of the finger at higher field strengths, and the differences among braille words are far subtler (Sanchez-Panchuelo et al., 2012). Even outside of S1, effects were weak and only partially overlapping with the other MVPA and univariate effects. These decoding results serve as a proof of principle that braille words can be decoded based on neural activity patterns, despite their high sensory similarity to each other and the dynamic nature of touch, but also suggest that these signatures are difficult to detect with conventional MVPA analyses.

In summary, we identified several neural signatures of orthographic processing in braille reading. Posterior-parietal and parieto-occipital cortices, including specifically the SMG, are sensitive to form-based orthographic properties of braille. The SMG showed sensitivity to uncontracted word length when participants read contracted braille, a possible signature of the processing of a dual (contracted and uncontracted) orthographic code. Activity in PPCs also distinguished between real and pseudowords. We hypothesize that PPCs plays a significant role in braille word recognition.

## APPENDIX

**Table A1.** List of Clusters in Whole-brain Univariate GLM and MVPA Decoding Accuracy Maps

	<i>Peak MNI Coordinates</i>			<i>Cluster Size</i>		<i>Peak p (FWE)</i>
	<i>x</i>	<i>y</i>	<i>z</i>	<i>Vertices</i>	<i>mm<sup>2</sup></i>	
<i>Univariate inanimate real word &gt; pseudoword</i>						
Left hemisphere						
Angular gyrus/superior angular gyrus	-40.5	-64.2	25.4	236	353.64	< .0001
Superior frontal sulcus	-21.1	24.2	39.2	122	288.87	< .0001
PC	-5.6	-52.8	24.3	104	246.69	.0002
Right hemisphere						
Angular gyrus/superior angular gyrus	49.9	-63.4	22.9	115	209.91	< .0001
PC	8	-55.1	31.6	68	168.98	< .0001
Anterior superior temporal gyrus	63.1	-13.8	-3.5	63	155.62	< .0001
<i>Univariate pseudoword &gt; inanimate real word</i>						
Left hemisphere						
SMG	-43.6	-40.5	40.7	371	580.58	< .0001
Fusiform gyrus/lateral occipito-temporal sulcus	-27.9	-44	-20.8	235	670.6	< .0001
Superior anterior insula sulcus	-27.9	25.6	-3.9	197	373.74	< .0001
Superior occipital gyrus/IPS	-25.7	-73.5	23.4	177	408.54	.0002
Inferior PCS	-46.4	3.6	26.1	87	185.78	.0003
Postcentral gyrus	-52.9	-21.2	53.4	84	176.93	.0003
Middle occipital sulcus	-31.4	-87.4	-2.6	74	185.42	< .0001
Superior insula sulcus	-39.5	-2.7	5.2	71	149.65	< .0001
Inferior frontal gyrus	-36.7	31.8	-0.5	66	124.56	< .0001
Anterior middle cingulate gyrus	-4.3	5.9	29.2	60	97.61	< .0001
Inferior PCS	-50.2	4.3	13.8	57	101.22	< .0001
Right hemisphere						
IPS	50.3	-23	46.8	1147	1760.17	< .0001
Superior anterior insula sulcus	35.3	20.8	-0.9	555	1059.41	< .0001
PCS/inferior frontal sulcus	43.8	5	25.1	312	608.95	< .0001
Middle occipital sulcus	24.1	-85.9	17.6	252	523.63	.0001
Inferior occipital sulcus/gyrus	44.9	-63.5	-12.3	189	358.21	< .0001
Inferior frontal sulcus	49.5	35.7	4.5	181	355.37	< .0001
Fusiform gyrus	33.9	-49.4	-18.9	170	513.92	< .0001
Supramarginal gyrus	55.8	-24.2	36.1	120	169.92	.0003
Calcarine sulcus	13.4	-77.5	5.2	86	284.05	< .0001
Superior frontal sulcus	29	-3.9	46.4	77	127.05	< .0001
Anterior middle cingulate gyrus	11.6	17.5	38.5	64	126.38	< .0001
Occipital pole	13.4	-92.1	5.9	50	162.42	.0006

**Table A1.** (continued)

	Peak MNI Coordinates			Cluster Size		Peak <i>p</i> (FWE)
	<i>x</i>	<i>y</i>	<i>z</i>	Vertices	mm <sup>2</sup>	
<i>Univariate animate real word &gt; pseudoword</i>						
Left hemisphere						
Precuneus	-6.3	-60.8	39.1	806	1556.34	< .0001
Angular gyrus	-42.6	-67.7	28.6	456	757.6	< .0001
Superior frontal gyrus	-16.1	46.2	40.4	45	106.76	.0002
Right hemisphere						
PC	7	-58.2	37	378	711.2	< .0001
Angular gyrus	51.2	-61.5	21.3	147	315.86	< .0001
Posterior middle cingulate gyrus	2.7	-16.7	37.1	48	111.68	.0002
Suborbital sulcus	7.2	52.7	-10.5	32	91.2	< .0001
<i>Univariate pseudoword &gt; animate real word</i>						
Left hemisphere						
Inferior PCS	-50.2	4.3	13.8	68	119.36	.0004
Right hemisphere						
Inferior PCS	44.9	5.4	26.1	152	300.78	< .0001
SMG	48.7	-32.8	43.7	146	187.39	< .0001
Anterior superior insula sulcus	32.9	25.4	7.9	121	190.5	< .0001
IPS	37.4	-40.5	36.4	105	99.67	< .0001
<i>Uncontracted word length effect</i>						
Left hemisphere						
SMG	-36.3	-34.6	37	221	353.38	< .0001
Right hemisphere						
IPS	32.3	-42.2	39.8	306	300.53	< .0001
SMG	57.1	-32.7	47.5	240	323.03	< .0001
<i>Dot count effect</i>						
Left hemisphere						
Central sulcus	-33.1	-27.4	48.3	113	204.23	.0004
Right hemisphere						
STS	46	-34	0.5	120	173.53	< .0001
<i>Negative frequency effect</i>						
Left hemisphere						
Inferior frontal sulcus	-38.2	10.6	24.4	140	291.41	.0014
Superior frontal gyrus	-4.4	46.4	40.8	109	298.92	< .0001
Superior occipital sulcus	-24.8	-79.6	19.8	74	162.49	.0007

**Table A1.** (continued)

	Peak MNI Coordinates			Cluster Size		Peak <i>p</i> (FWE)
	<i>x</i>	<i>y</i>	<i>z</i>	Vertices	mm <sup>2</sup>	
Right hemisphere						
Fusiform gyrus	37.2	-36.2	-24.9	139	404.71	< .0001
Middle temporal gyrus	63.3	-27.5	-17.9	93	269.45	.0001
MVPA decoding (inanimate real words vs. pseudowords)						
Left hemisphere						
Angular gyrus	-28.7	-66.4	32.4	436	701.68	< .0001
Inferior PCS	-50.8	4.6	21.2	378	762.69	.0001
Lateral occipito-temporal sulcus/inferior temporal gyrus	-44.3	-53.8	-10.4	206	368.37	< .0001
Posterior STS	-49.1	-55.1	7.7	110	172.12	< .0001
Middle occipital gyrus	-39.3	-78.1	9.8	78	169.72	< .0001
Right hemisphere						
SMG	54.8	-44.5	42.1	627	805.53	< .0001
Inferior frontal sulcus	49	3.6	32.1	428	883.09	< .0001
IPS	23.1	-61.3	39.2	237	299.23	< .0001
Anterior superior insula sulcus	31	25.1	6.1	60	93.94	.0002

The table only includes clusters passing the permutation-based correction controlling for FWER, with cluster-forming threshold of  $p < .01$  and cluster-wise threshold of  $p < .05$ . IPS = intraparietal sulcus; PC = precuneus; PCS = precentral sulcus; SMG = supramarginal gyrus; STS = superior temporal sulcus.

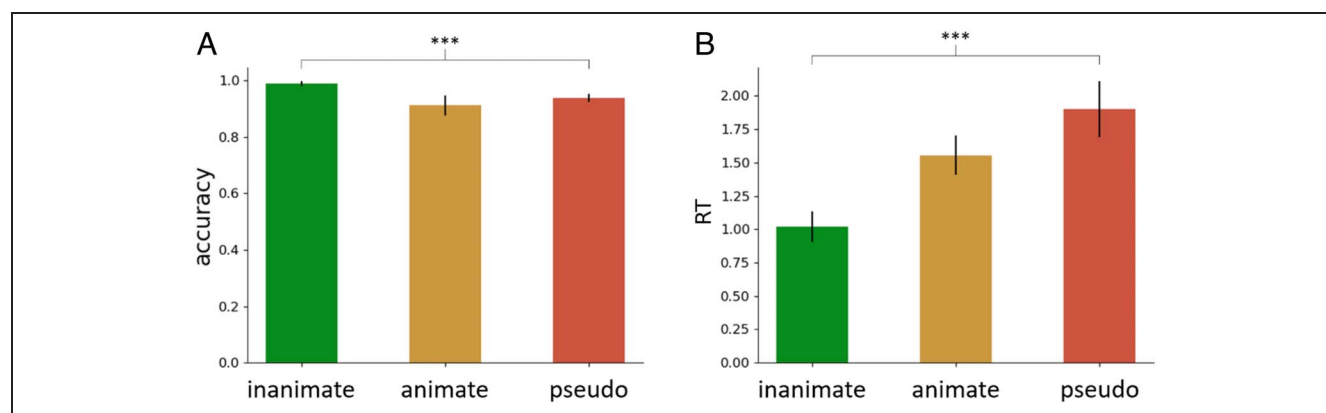


**Figure A1.** Behavioral results of the fMRI task. (A) Accuracy. (B) RT. \*\*\* $p < .001$ .

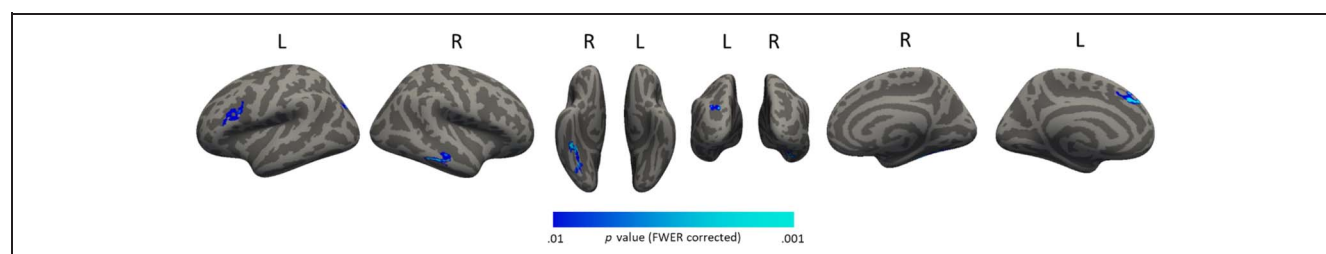


**Figure A2.** The negative effect of log word frequency, with less activity for higher frequency words. The map was cluster-based permutation corrected to control the FWER. The cluster-forming threshold was uncorrected  $p < .01$ , and the cluster-wise FWER threshold was  $p < .05$ .

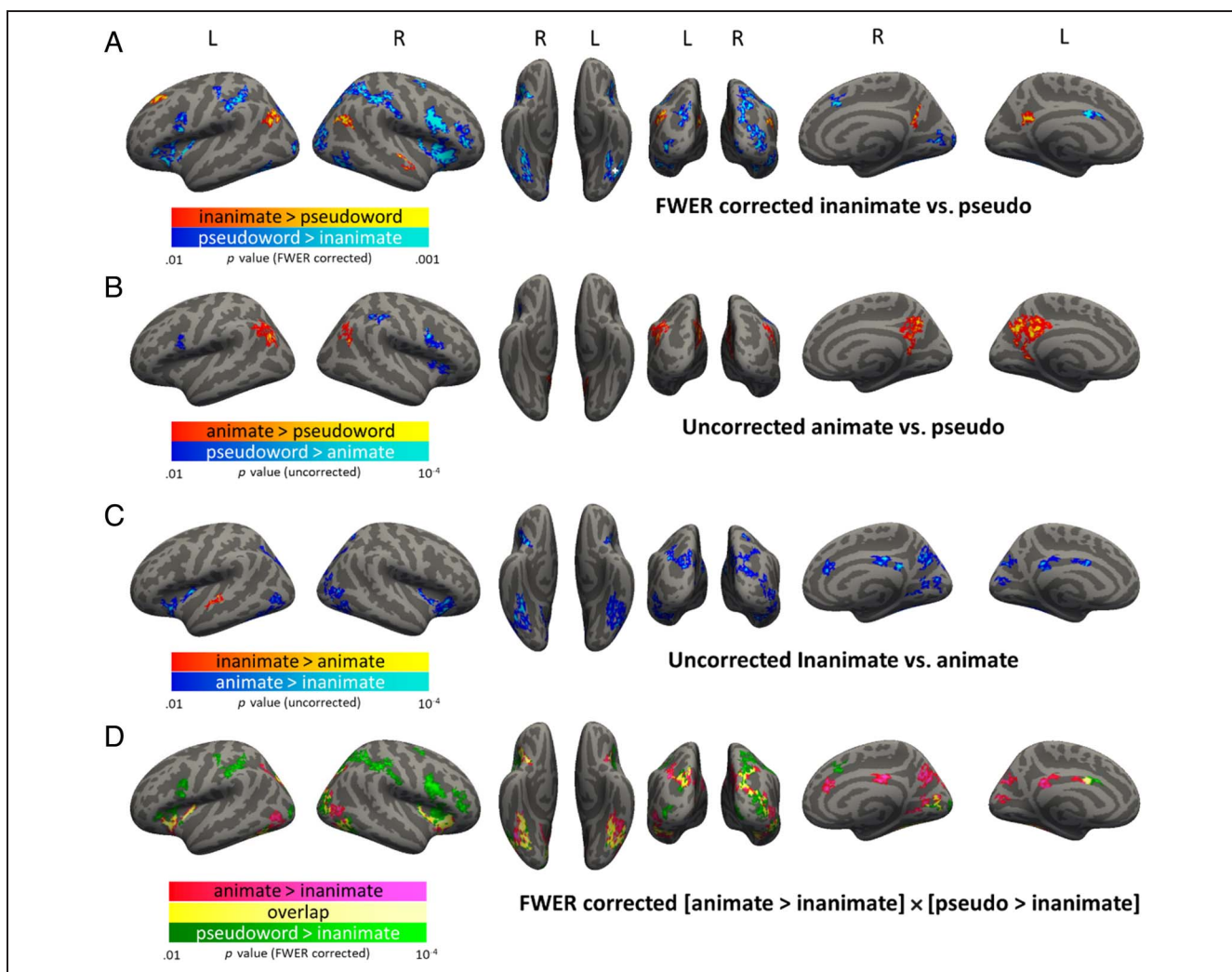


**Figure A3.** (A) The univariate contrast between inanimate real words and pseudowords, the same as Figure 2A. (B) The univariate contrasts between animate real words and pseudowords, without FWER correction. (C) The univariate contrasts between inanimate and animate real words, without FWER correction. (D) An overlay of two contrasts: “animate > inanimate real words” (pink) and “pseudowords > inanimate real words” (green), with the overlap between the two maps colored yellow. This map had undergone permutation-based FWER correction, with cluster-forming threshold of  $p < .01$  and cluster-wise  $p < .05$ .

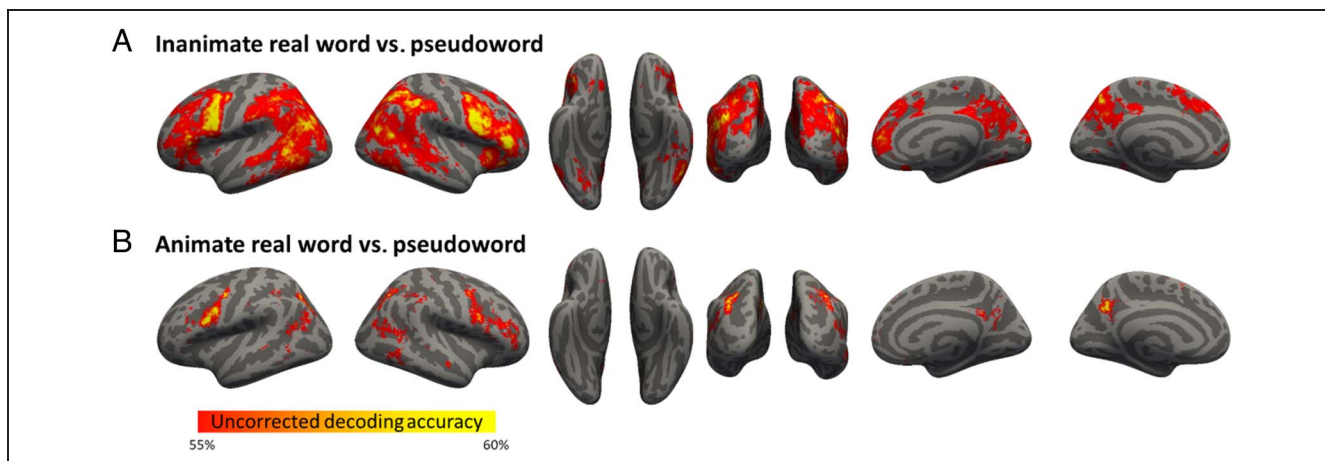


**Figure A4.** Uncorrected MVPA decoding accuracy (A) between inanimate real words and pseudowords, and (B) between animate real words and pseudowords. Note that Figure 2B was derived by masking Figure A4A with clusters that passed the permutation-based FWER correction.

**Figure A5.** Ventral view of the left hemisphere in five maps in which exploratory thresholds (uncorrected  $p < .05$ ) were applied. From left to right: real word > pseudoword contrast, pseudoword > real word contrast, real word versus pseudoword MVPA decoding, letter length effect, negative frequency effect. Only clusters with greater than 50 vertices are shown. No permutation-based cluster correction was performed. “Real word” refers to inanimate real word.

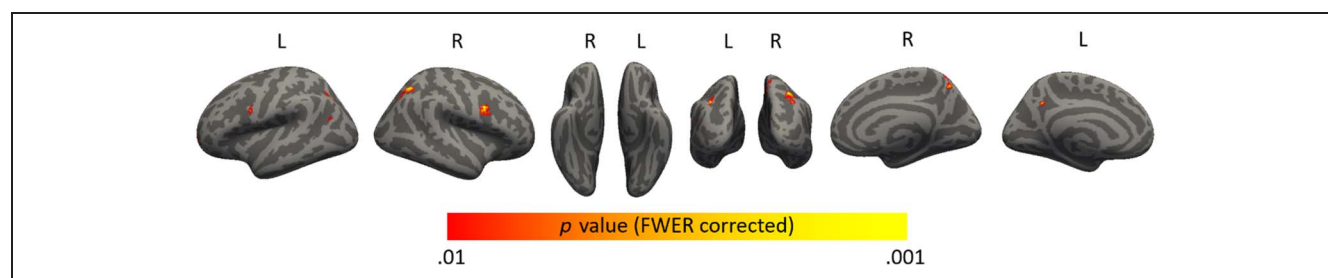
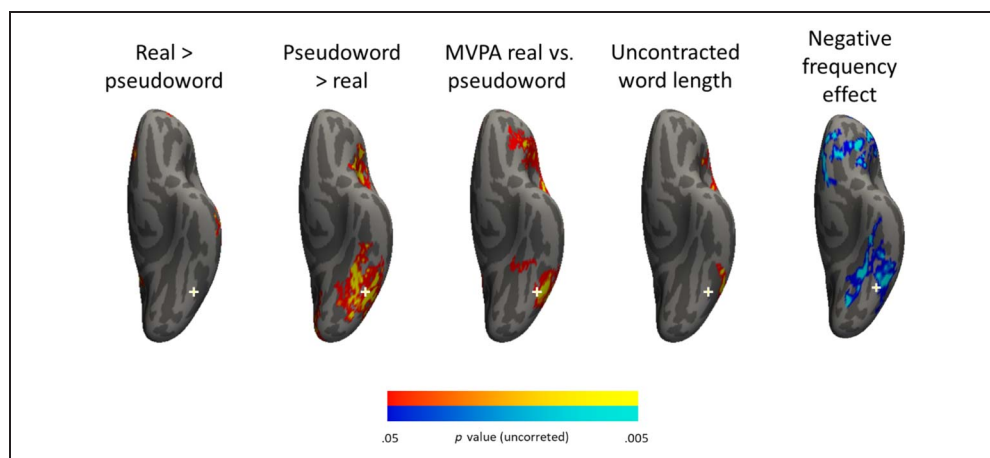


**Figure A6.** Split-half MVPA searchlight correlation analysis. The brain map shows cortical regions where, averaged across all inanimate real words, the similarity between any inanimate real word and itself was greater than between that word and all other inanimate real words in the stimulus set. The map underwent cluster-based permutation correction to control the FWER. The cluster-forming threshold was uncorrected  $p < .01$ , and the cluster-wise FWER threshold was  $p < .05$ .

## Acknowledgments

We are grateful to the participants and the Baltimore blind community without whose support this research would not be possible. We thank Dr. Judy Kim and Lindsay Yazzolino for input on the design of this project; Brianna Alheimer for help with data collection; Dr. Robert Englebretson for valuable intellectual input regarding earlier drafts of this article.

Reprint requests should be sent to Yun-Fei Liu, Department of Psychological and Brain Sciences, Johns Hopkins University, 3400 N Charles St., Ames Hall 232, Baltimore, MD 21218–2625, United States, or via e-mail: [yliu291@jhu.edu](mailto:yliu291@jhu.edu).

## Data Availability Statement

Behavioral data, experiment stimuli, and the script for the generation and presentation of the stimuli are available in an OSF repository: <https://osf.io/tnbd5/>. Due to limitations of IRB approval, Neuroimaging data cannot be shared.

## Author Contributions

Yun-Fei Liu: Conceptualization; Data curation; Formal analysis; Investigation; Methodology; Project administration; Visualization; Writing—Original draft; Writing—Review & editing. Brenda Rapp: Conceptualization; Writing—Review & editing. Marina Bedny: Conceptualization;

Funding acquisition; Investigation; Methodology; Resources; Software; Supervision; Writing—Original draft; Writing—Review & editing.

## Funding Information

National Eye Institute (<https://dx.doi.org/10.13039/1000000053>), grant number: R01EY033340.

## Diversity in Citation Practices

Retrospective analysis of the citations in every article published in this journal from 2010 to 2021 reveals a persistent pattern of gender imbalance: Although the proportions of authorship teams (categorized by estimated gender identification of first author/last author) publishing in the *Journal of Cognitive Neuroscience (JoCN)* during this period were  $M(\text{an})/M = .407$ ,  $W(\text{oman})/M = .32$ ,  $M/W = .115$ , and  $W/W = .159$ , the comparable proportions for the articles that these authorship teams cited were  $M/M = .549$ ,  $W/M = .257$ ,  $M/W = .109$ , and  $W/W = .085$  (Postle and Fulvio, *JoCN*, 34:1, pp. 1–3). Consequently, *JoCN* encourages all authors to consider gender balance explicitly when selecting which articles to cite and gives them the opportunity to report their article’s gender citation balance.

## REFERENCES

- Baayen, R. H., Davidson, D. J., & Bates, D. M. (2008). Mixed-effects modeling with crossed random effects for subjects and items. *Journal of Memory and Language*, *59*, 390–412. <https://doi.org/10.1016/j.jml.2007.12.005>
- Bai, J., Shi, J., Jiang, Y., He, S., & Weng, X. (2011). Chinese and Korean characters engage the same visual word form area in proficient early Chinese–Korean bilinguals. *PLoS One*, *6*, e22765. <https://doi.org/10.1371/journal.pone.0022765>, PubMed: 21818386
- Bauer, C., Yazzolino, L., Hirsch, G., Cattaneo, Z., Vecchi, T., & Merabet, L. B. (2015). Neural correlates associated with superior tactile symmetry perception in the early blind. *Cortex*, *63*, 104–117. <https://doi.org/10.1016/j.cortex.2014.08.003>, PubMed: 25243993
- Bedny, M., Pascual-Leone, A., Dodell-Feder, D., Fedorenko, E., & Saxe, R. (2011). Language processing in the occipital cortex of congenitally blind adults. *Proceedings of the National Academy of Sciences, U.S.A.*, *108*, 4429–4434. <https://doi.org/10.1073/pnas.1014818108>, PubMed: 21368161
- Blank, I., Kanwisher, N., & Fedorenko, E. (2014). A functional dissociation between language and multiple-demand systems revealed in patterns of BOLD signal fluctuations. *Journal of Neurophysiology*, *112*, 1105–1118. <https://doi.org/10.1152/jn.00884.2013>, PubMed: 24872535
- Bodegård, A., Geyer, S., Grefkes, C., Zilles, K., & Roland, P. E. (2001). Hierarchical processing of tactile shape in the human brain. *Neuron*, *31*, 317–328. [https://doi.org/10.1016/S0896-6273\(01\)00362-2](https://doi.org/10.1016/S0896-6273(01)00362-2), PubMed: 11502261
- Bohlhalter, S., Fretz, C., & Weder, B. (2002). Hierarchical versus parallel processing in tactile object recognition: A behavioural–neuroanatomical study of a perceptive tactile agnosia. *Brain*, *125*, 2537–2548. <https://doi.org/10.1093/brain/awf245>, PubMed: 12390978
- Bouhali, F., Bézagu, Z., Dehaene, S., & Cohen, L. (2019). A mesial-to-lateral dissociation for orthographic processing in the visual cortex. *Proceedings of the National Academy of Sciences, U.S.A.*, *116*, 21936–21946. <https://doi.org/10.1073/pnas.1904184116>, PubMed: 31591198
- Brysbaert, M., Mander, P., & Keuleers, E. (2018). The word frequency effect in word processing: An updated review. *Current Directions in Psychological Science*, *27*, 45–50. <https://doi.org/10.1177/0963721417727521>
- Büchel, C., Price, C., & Friston, K. (1998). A multimodal language region in the ventral visual pathway. *Nature*, *394*, 274–277. <https://doi.org/10.1038/28389>, PubMed: 9685156
- Burks, J. D., Boettcher, L. B., Conner, A. K., Glenn, C. A., Bonney, P. A., Baker, C. M., et al. (2017). White matter connections of the inferior parietal lobule: A study of surgical anatomy. *Brain and Behavior*, *7*, e00640. <https://doi.org/10.1002/brb3.640>, PubMed: 28413699
- Burton, H., Diamond, J., & McDermott, K. (2003). Dissociating cortical regions activated by semantic and phonological tasks: A fMRI study in blind and sighted people. *Journal of Neurophysiology*, *90*, 1965–1982. <https://doi.org/10.1152/jn.00279.2003>, PubMed: 12789013
- Burton, H., MacLeod, A.-M., Videen, T., & Raichle, M. (1997). Multiple foci in parietal and frontal cortex activated by rubbing embossed grating patterns across fingerpads: A positron emission tomography study in humans. *Cerebral Cortex*, *7*, 3–17. <https://doi.org/10.1093/cercor/7.1.3>, PubMed: 9023428
- Burton, H., Sinclair, R. J., & Agato, A. (2012). Recognition memory for braille or spoken words: An fMRI study in early blind. *Brain Research*, *1438*, 22–34. <https://doi.org/10.1016/j.brainres.2011.12.032>, PubMed: 22251836
- Burton, H., Snyder, A., Diamond, J., & Raichle, M. (2002). Adaptive changes in early and late blind: A fMRI study of verb generation to heard nouns. *Journal of Neurophysiology*, *88*, 3359–3371. <https://doi.org/10.1152/jn.00129.2002>, PubMed: 12466452
- Caramazza, A., Capasso, R., & Miceli, G. (1996). The role of the graphemic buffer in reading. *Cognitive Neuropsychology*, *13*, 673–698. <https://doi.org/10.1080/026432996381881>
- Carreiras, M., Quiñones, I., Hernández-Cabrera, J. A., & Duñabeitia, J. A. (2015). Orthographic coding: Brain activation for letters, symbols, and digits. *Cerebral Cortex*, *25*, 4748–4760. <https://doi.org/10.1093/cercor/bhu163>, PubMed: 25077489
- Catani, M., Jones, D. K., & Ffytche, D. H. (2005). Perisylvian language networks of the human brain. *Annals of Neurology*, *57*, 8–16. <https://doi.org/10.1002/ana.20319>, PubMed: 15597383
- Chang, C.-C., & Lin, C.-J. (2011). LIBSVM: A library for support vector machines. *ACM Transactions on Intelligent Systems and Technology*, *2*, 1–27. <https://doi.org/10.1145/1961189.1961199>
- Chang, C. H., Pallier, C., Wu, D. H., Nakamura, K., Jobert, A., Kuo, W.-J., et al. (2015). Adaptation of the human visual system to the statistics of letters and line configurations. *Nature*, *520*, 428–440. <https://doi.org/10.1038/nature1467-019-13634-z>, PubMed: 26190404
- Chen, L., Wassermann, D., Abrams, D. A., Kochalka, J., Gallardo-Diez, G., & Menon, V. (2019). The visual word form area (VWFA) is part of both language and attention circuitry. *Nature Communications*, *10*, 5601. <https://doi.org/10.1038/s41467-019-13634-z>, PubMed: 31811149
- Chivukula, S., Zhang, C. Y., Aflalo, T., Jafari, M., Pejsa, K., Pouratian, N., et al. (2021). Neural encoding of actual and imagined touch within human posterior parietal cortex. *eLife*, *10*, e61646. <https://doi.org/10.7554/eLife.61646>, PubMed: 33647233
- Choi, W., Desai, R. H., & Henderson, J. M. (2014). The neural substrates of natural reading: A comparison of normal and nonword text using eyetracking and fMRI. *Frontiers in Human Neuroscience*, *8*, 1024. <https://doi.org/10.3389/fnhum.2014.01024>, PubMed: 25566039
- Church, J. A., Balota, D. A., Petersen, S. E., & Schlaggar, B. L. (2011). Manipulation of length and lexicality localizes the functional neuroanatomy of phonological processing in adult readers. *Journal of Cognitive Neuroscience*, *23*, 1475–1493. <https://doi.org/10.1162/jocn.2010.21515>, PubMed: 20433237
- Cohen, L., Dehaene, S., Vinckier, F., Jobert, A., & Montavont, A. (2008). Reading normal and degraded words: Contribution of the dorsal and ventral visual pathways. *Neuroimage*, *40*, 353–366. <https://doi.org/10.1016/j.neuroimage.2007.11.036>, PubMed: 18182174
- Cohen, L., Lehericy, S., Chochon, F., Lemer, C., Rivaud, S., & Dehaene, S. (2002). Language-specific tuning of visual cortex? Functional properties of the visual word form area. *Brain*, *125*, 1054–1069. <https://doi.org/10.1093/brain/awf094>, PubMed: 11960895
- Coltheart, V., Patterson, K., & Leahy, J. (1994). When a ROWS is a ROSE: Phonological effects in written word comprehension. *Quarterly Journal of Experimental Psychology*, *47*, 917–955. <https://doi.org/10.1080/14640749408401102>
- Dale, A. M., Fischl, B., & Sereno, M. I. (1999). Cortical surface-based analysis: I. Segmentation and surface reconstruction. *Neuroimage*, *9*, 179–194. <https://doi.org/10.1006/nimg.1998.0395>, PubMed: 9931268
- Davies, M. (2008). *The Corpus of Contemporary American English (COCA): 560 million words, 1990–present*. Retrieved from <https://www.english-corpora.org/coca/>.
- Debowska, W., Wolak, T., Nowicka, A., Kozak, A., Szwed, M., & Kossut, M. (2016). Functional and structural neuroplasticity

- induced by short-term tactile training based on braille reading. *Frontiers in Neuroscience*, *10*, 460. <https://doi.org/10.3389/fnins.2016.00460>, PubMed: 27790087
- Dehaene, S., & Cohen, L. (2007). Cultural recycling of cortical maps. *Neuron*, *56*, 384–398. <https://doi.org/10.1016/j.neuron.2007.10.004>, PubMed: 17964253
- Dehaene, S., & Cohen, L. (2011). The unique role of the visual word form area in reading. *Trends in Cognitive Sciences*, *15*, 254–262. <https://doi.org/10.1016/j.tics.2011.04.003>, PubMed: 21592844
- Dehaene, S., Cohen, L., Sigman, M., & Vinckier, F. (2005). The neural code for written words: A proposal. *Trends in Cognitive Sciences*, *9*, 335–341. <https://doi.org/10.1016/j.tics.2005.05.004>, PubMed: 15951224
- Dehaene, S., Le Clec'H, G., Poline, J.-B., Le Bihan, D., & Cohen, L. (2002). The visual word form area: A prelexical representation of visual words in the fusiform gyrus. *NeuroReport*, *13*, 321–325. <https://doi.org/10.1097/00001756-200203040-00015>, PubMed: 11930131
- Dehaene, S., Pegado, F., Braga, L. W., Ventura, P., Filho, G. N., Jobert, A., et al. (2010). How learning to read changes the cortical networks for vision and language. *Science*, *330*, 1359–1364. <https://doi.org/10.1126/science.1194140>, PubMed: 21071632
- Deschamps, I., Baum, S. R., & Gracco, V. L. (2014). On the role of the supramarginal gyrus in phonological processing and verbal working memory: Evidence from rTMS studies. *Neuropsychologia*, *53*, 39–46. <https://doi.org/10.1016/j.neuropsychologia.2013.10.015>, PubMed: 24184438
- Dietz, N. A. E., Jones, K. M., Gareau, L., Zeffiro, T. A., & Eden, G. F. (2005). Phonological decoding involves left posterior fusiform gyrus. *Human Brain Mapping*, *26*, 81–93. <https://doi.org/10.1002/hbm.20122>, PubMed: 15934062
- Dzięciel-Fivet, G., Plewko, J., Szczerbiński, M., Marchewka, A., Szwed, M., & Jednoróg, K. (2021). Neural network for braille reading and the speech-reading convergence in the blind: Similarities and differences to visual reading. *Neuroimage*, *231*, 117851. <https://doi.org/10.1016/j.neuroimage.2021.117851>, PubMed: 33582273
- Eklund, A., Knutsson, H., & Nichols, T. E. (2019). Cluster failure revisited: Impact of first level design and physiological noise on cluster false positive rates. *Human Brain Mapping*, *40*, 2017–2032. <https://doi.org/10.1002/hbm.24350>, PubMed: 30318709
- Eklund, A., Nichols, T. E., & Knutsson, H. (2016). Cluster failure: Why fMRI inferences for spatial extent have inflated false-positive rates. *Proceedings of the National Academy of Sciences, U.S.A.*, *113*, 7900–7905. <https://doi.org/10.1073/pnas.1602413113>, PubMed: 27357684
- Elli, G. V., Lane, C., & Bedny, M. (2019). A double dissociation in sensitivity to verb and noun semantics across cortical networks. *Cerebral Cortex*, *29*, 4803–4817. <https://doi.org/10.1093/cercor/bhz014>, PubMed: 30767007
- Fedorenko, E., Scott, T. L., Brunner, P., Coon, W. G., Pritchett, B., Schalk, G., et al. (2016). Neural correlate of the construction of sentence meaning. *Proceedings of the National Academy of Sciences, U.S.A.*, *113*, E6256–E6262. <https://doi.org/10.1073/pnas.1612132113>, PubMed: 27671642
- Fedorenko, E., & Varley, R. (2016). Language and thought are not the same thing: Evidence from neuroimaging and neurological patients. *Annals of the New York Academy of Sciences*, *1369*, 132–153. <https://doi.org/10.1111/nyas.13046>, PubMed: 27096882
- Fiebach, C. J., Friederici, A. D., Müller, K., & von Cramon, D. Y. (2002). fMRI evidence for dual routes to the mental lexicon in visual word recognition. *Journal of Cognitive Neuroscience*, *14*, 11–23. <https://doi.org/10.1162/089892902317205285>, PubMed: 11798383
- Fischer-Baum, S., Bruggemann, D., Gallego, I. F., Li, D. S. P., & Tamez, E. R. (2017). Decoding levels of representation in reading: A representational similarity approach. *Cortex*, *90*, 88–102. <https://doi.org/10.1016/j.cortex.2017.02.017>, PubMed: 28384482
- Fischer-Baum, S., & Englebretson, R. (2016). Orthographic units in the absence of visual processing: Evidence from sublexical structure in braille. *Cognition*, *153*, 161–174. <https://doi.org/10.1016/j.cognition.2016.03.021>, PubMed: 27206313
- Fischer-Baum, S., & Rapp, B. (2014). The analysis of perseverations in acquired dysgraphia reveals the internal structure of orthographic representations. *Cognitive Neuropsychology*, *31*, 237–265. <https://doi.org/10.1080/02643294.2014.880676>, PubMed: 24499188
- Forster, K. I., & Chambers, S. M. (1973). Lexical access and naming time. *Journal of Verbal Learning and Verbal Behavior*, *12*, 627–635. [https://doi.org/10.1016/S0022-5371\(73\)80042-8](https://doi.org/10.1016/S0022-5371(73)80042-8)
- Frey, S., Campbell, J. S. W., Pike, G. B., & Petrides, M. (2008). Dissociating the human language pathways with high angular resolution diffusion fiber tractography. *Journal of Neuroscience*, *28*, 11435–11444. <https://doi.org/10.1523/JNEUROSCI.2388-08.2008>, PubMed: 18987180
- Friederici, A., & Gierhan, S. (2013). The language network. *Current Opinion in Neurobiology*, *23*, 250–254. <https://doi.org/10.1016/j.conb.2012.10.002>, PubMed: 23146876
- Friederici, A., Rueschemeyer, S.-A., Hahne, A., & Fiebach, C. J. (2003). The role of left inferior frontal and superior temporal cortex in sentence comprehension: Localizing syntactic and semantic processes. *Cerebral Cortex*, *13*, 170–177. <https://doi.org/10.1093/cercor/13.2.170>, PubMed: 12507948
- Glasser, M. F., Sotiropoulos, S. N., Wilson, J. A., Coalson, T. S., Fischl, B., Andersson, J. L., et al. (2013). The minimal preprocessing pipelines for the human connectome project. *Neuroimage*, *80*, 105–124. <https://doi.org/10.1016/j.neuroimage.2013.04.127>, PubMed: 23668970
- Goswami, U., Ziegler, J. C., Dalton, L., & Schneider, W. (2001). Pseudohomophone effects and phonological recoding procedures in reading development in English and German. *Journal of Memory and Language*, *45*, 648–664. <https://doi.org/10.1006/jmla.2001.2790>
- Graves, W. W., Desai, R., Humphries, C., Seidenberg, M. S., & Binder, J. R. (2010). Neural systems for reading aloud: A multiparametric approach. *Cerebral Cortex*, *20*, 1799–1815. <https://doi.org/10.1093/cercor/bhp245>, PubMed: 19920057
- Hagler, D. J., Saygin, A. P., & Sereno, M. I. (2006). Smoothing and cluster thresholding for cortical surface-based group analysis of fMRI data. *Neuroimage*, *33*, 1093–1103. <https://doi.org/10.1016/j.neuroimage.2006.07.036>, PubMed: 17011792
- Hagoort, P., Indefrey, P., Brown, C., Herzog, H., Steinmetz, H., & Seitz, R. J. (1999). The neural circuitry involved in the reading of German words and pseudowords: A PET study. *Journal of Cognitive Neuroscience*, *11*, 383–398. <https://doi.org/10.1162/089892999563490>, PubMed: 10471847
- Haxby, J. V., Connolly, A. C., & Guntupalli, J. S. (2014). Decoding neural representational spaces using multivariate pattern analysis. *Annual Review of Neuroscience*, *37*, 435–456. <https://doi.org/10.1146/annurev-neuro-062012-170325>, PubMed: 25002277
- Heim, S., Alter, K., Ischebeck, A. K., Amunts, K., Eickhoff, S. B., Mohlberg, H., et al. (2005). The role of the left Brodmann's areas 44 and 45 in reading words and pseudowords. *Cognitive Brain Research*, *25*, 982–993. <https://doi.org/10.1016/j.cogbrainres.2005.09.022>, PubMed: 16310346
- Ischebeck, A., Indefrey, P., Usui, N., Nose, I., Hellwig, F., & Taira, M. (2004). Reading in a regular orthography: An fMRI

- study investigating the role of visual familiarity. *Journal of Cognitive Neuroscience*, *16*, 727–741. <https://doi.org/10.1162/089892904970708>, PubMed: 15200701
- Jitsuishi, T., Hirono, S., Yamamoto, T., Kitajo, K., Iwadata, Y., & Yamaguchi, A. (2020). White matter dissection and structural connectivity of the human vertical occipital fasciculus to link vision-associated brain cortex. *Scientific Reports*, *10*, 820. <https://doi.org/10.1038/s41598-020-57837-7>, PubMed: 31965011
- Jobard, G., Crivello, F., & Tzourio-Mazoyer, N. (2003). Evaluation of the dual route theory of reading: A metanalysis of 35 neuroimaging studies. *Neuroimage*, *20*, 693–712. [https://doi.org/10.1016/s1053-8119\(03\)00343-4](https://doi.org/10.1016/s1053-8119(03)00343-4), PubMed: 14568445
- Kim, J. S., Kanjlia, S., Merabet, L. B., & Bedny, M. (2017). Development of the visual word form area requires visual experience: Evidence from blind braille readers. *Journal of Neuroscience*, *37*, 11495–11504. <https://doi.org/10.1523/jneurosci.0997-17.2017>, PubMed: 29061700
- Kriegeskorte, N., Goebel, R., & Bandettini, P. (2006). Information-based functional brain mapping. *Proceedings of the National Academy of Sciences, U.S.A.*, *103*, 3863–3868. <https://doi.org/10.1073/pnas.0600244103>, PubMed: 16537458
- Kronbichler, M., Hutzler, F., Wimmer, H., Mair, A., Staffen, W., & Ladurner, G. (2004). The visual word form area and the frequency with which words are encountered: Evidence from a parametric fMRI study. *Neuroimage*, *21*, 946–953. <https://doi.org/10.1016/j.neuroimage.2003.10.021>, PubMed: 15006661
- Kuo, W.-J., Yeh, T.-C., Lee, C.-Y., Wu, Y. u.-T., Chou, C.-C., Ho, L.-T., et al. (2003). Frequency effects of Chinese character processing in the brain: An event-related fMRI study. *Neuroimage*, *18*, 720–730. [https://doi.org/10.1016/S1053-8119\(03\)00015-6](https://doi.org/10.1016/S1053-8119(03)00015-6), PubMed: 12667849
- Lane, C., Kanjlia, S., Omaki, A., & Bedny, M. (2015). “Visual” cortex of congenitally blind adults responds to syntactic movement. *Journal of Neuroscience*, *35*, 12859–12868. <https://doi.org/10.1523/jneurosci.1256-15.2015>, PubMed: 26377472
- Lane, C., Kanjlia, S., Richardson, H., Fulton, A., Omaki, A., & Bedny, M. (2017). Reduced left lateralization of language in congenitally blind individuals. *Journal of Cognitive Neuroscience*, *29*, 65–78. [https://doi.org/10.1162/jocn\\_a\\_01045](https://doi.org/10.1162/jocn_a_01045), PubMed: 27647280
- Leinenger, M. (2014). Phonological coding during reading. *Psychological Bulletin*, *140*, 1534–1555. <https://doi.org/10.1037/a0037830>, PubMed: 25150679
- Leo, A., Bernardi, G., Handjaras, G., Bonino, D., Ricciardi, E., & Pietrini, P. (2012). Increased BOLD variability in the parietal cortex and enhanced parieto-occipital connectivity during tactile perception in congenitally blind individuals. *Neural Plasticity*, *2012*, 720278. <https://doi.org/10.1155/2012/720278>, PubMed: 22792493
- Li Hegner, Y., Lee, Y., Grodd, W., & Braun, C. (2010). Comparing tactile pattern and vibrotactile frequency discrimination: A human fMRI study. *Journal of Neurophysiology*, *103*, 3115–3122. <https://doi.org/10.1152/jn.00940.2009>, PubMed: 20457848
- Lin, N., Yu, X., Zhao, Y., & Zhang, M. (2016). Functional anatomy of recognition of Chinese multi-character words: Convergent evidence from effects of transposable nonwords, lexicality, and word frequency. *PLoS One*, *11*, e0149583. <https://doi.org/10.1371/journal.pone.0149583>, PubMed: 26901644
- Liu, C., Zhang, W.-T., Tang, Y.-Y., Mai, X.-Q., Chen, H.-C., Tardif, T., et al. (2008). The visual word form area: Evidence from an fMRI study of implicit processing of Chinese characters. *Neuroimage*, *40*, 1350–1361. <https://doi.org/10.1016/j.neuroimage.2007.10.014>, PubMed: 18272399
- Loiotile, R., Lane, C., Omaki, A., & Bedny, M. (2020). Enhanced performance on a sentence comprehension task in congenitally blind adults. *Language, Cognition and Neuroscience*, *35*, 1010–1023. <https://doi.org/10.1080/23273798.2019.1706753>, PubMed: 33043067
- Mahmoudi, A., Takerkart, S., Regragui, F., Boussaoud, D., & Brovelli, A. (2012). Multivoxel pattern analysis for fMRI data: A review. *Computational and Mathematical Methods in Medicine*, *2012*, 961257. <https://doi.org/10.1155/2012/961257>, PubMed: 23401720
- Mano, Q. R., Humphries, C., Desai, R. H., Seidenberg, M. S., Osmon, D. C., Stengel, B. C., et al. (2012). The role of left occipitotemporal cortex in reading: Reconciling stimulus, task, and lexicality effects. *Cerebral Cortex*, *23*, 988–1001. <https://doi.org/10.1093/cercor/bhs093>, PubMed: 22505661
- Margulies, D. S., & Petrides, M. (2013). Distinct parietal and temporal connectivity profiles of ventrolateral frontal areas involved in language production. *Journal of Neuroscience*, *33*, 16846–16852. <https://doi.org/10.1523/jneurosci.2259-13.2013>, PubMed: 24133284
- Marshall, J. C., & Newcombe, F. (1973). Patterns of paralexia: A psycholinguistic approach. *Journal of Psycholinguistic Research*, *2*, 175–199. <https://doi.org/10.1007/BF01067101>, PubMed: 4795473
- McCandliss, B. D., Cohen, L., & Dehaene, S. (2003). The visual word form area: Expertise for reading in the fusiform gyrus. *Trends in Cognitive Sciences*, *7*, 293–299. [https://doi.org/10.1016/S1364-6613\(03\)00134-7](https://doi.org/10.1016/S1364-6613(03)00134-7), PubMed: 12860187
- Mechelli, A., Gorno-Tempini, M. L., & Price, C. J. (2003). Neuroimaging studies of word and pseudoword reading: Consistencies, inconsistencies, and limitations. *Journal of Cognitive Neuroscience*, *15*, 260–271. <https://doi.org/10.1162/089892903321208196>, PubMed: 12676063
- Millar, S. (1997). *Reading by touch*. Routledge.
- Misaki, M., Kim, Y., Bandettini, P. A., & Kriegeskorte, N. (2010). Comparison of multivariate classifiers and response normalizations for pattern-information fMRI. *Neuroimage*, *53*, 103–118. <https://doi.org/10.1016/j.neuroimage.2010.05.051>, PubMed: 20580933
- Mohan, H., de Haan, R., Mansvelder, H. D., & de Kock, C. P. J. (2018). The posterior parietal cortex as integrative hub for whisker sensorimotor information. *Neuroscience*, *368*, 240–245. <https://doi.org/10.1016/j.neuroscience.2017.06.020>, PubMed: 28642168
- Monsell, S., Doyle, M. C., & Haggard, P. N. (1989). Effects of frequency on visual word recognition tasks: Where are they? *Journal of Experimental Psychology: General*, *118*, 43–71. <https://doi.org/10.1037/0096-3445.118.1.43>, PubMed: 2522506
- Moulton, E., Bouhali, F., Monzalvo, K., Poupon, C., Zhang, H., Dehaene, S., et al. (2019). Connectivity between the visual word form area and the parietal lobe improves after the first year of reading instruction: A longitudinal MRI study in children. *Brain Structure and Function*, *224*, 1519–1536. <https://doi.org/10.1007/s00429-019-01855-3>, PubMed: 30840149
- Nakamura, K., Dehaene, S., Jobert, A., Le Bihan, D., & Kouider, S. (2005). Subliminal convergence of kanji and kana words: Further evidence for functional parcellation of the posterior temporal cortex in visual word perception. *Journal of Cognitive Neuroscience*, *17*, 954–968. <https://doi.org/10.1162/0898929054021166>, PubMed: 15969912
- Nakamura, K., Kuo, W.-J., Pegado, F., Cohen, L., Tzeng, O. J. L., & Dehaene, S. (2012). Universal brain systems for recognizing word shapes and handwriting gestures during reading. *Proceedings of the National Academy of Sciences*,

- U.S.A., 109, 20762–20767. <https://doi.org/10.1073/pnas.1217749109>, PubMed: 23184998
- Nichols, T. E., & Holmes, A. P. (2002). Nonparametric permutation tests for functional neuroimaging: A primer with examples. *Human Brain Mapping*, 15, 1–25. <https://doi.org/10.1002/hbm.1058>, PubMed: 11747097
- Norman, K. A., Polyn, S. M., Detre, G. J., & Haxby, J. V. (2006). Beyond mind-reading: Multi-voxel pattern analysis of fMRI data. *Trends in Cognitive Sciences*, 10, 424–430. <https://doi.org/10.1016/j.tics.2006.07.005>, PubMed: 16899397
- Parker, G. J. M., Luzzi, S., Alexander, D. C., Wheeler-Kingshott, C. A. M., Ciccarelli, O., & Lambon Ralph, M. A. (2005). Lateralization of ventral and dorsal auditory-language pathways in the human brain. *Neuroimage*, 24, 656–666. <https://doi.org/10.1016/j.neuroimage.2004.08.047>, PubMed: 15652301
- Pedregosa, F., Varoquaux, G., Gramfort, A., Michel, V., Thirion, B., Grisel, O., et al. (2011). Scikit-learn: Machine learning in python. *Journal of Machine Learning Research*, 12, 2825–2830. <https://doi.org/10.5555/1953048.2078195>
- Peelen, M. V., He, C., Han, Z., Caramazza, A., & Bi, Y. (2014). Nonvisual and visual object shape representations in occipitotemporal cortex: Evidence from congenitally blind and sighted adults. *Journal of Neuroscience*, 34, 163–170. <https://doi.org/10.1523/JNEUROSCI.1114-13.2014>, PubMed: 24381278
- Pinheiro, J., Bates, D., & R Core Team. (2022). *Nlme: Linear and nonlinear mixed effects models* (Version R package version 3.1–161). Retrieved from <https://CRAN.R-project.org/package=nlme>.
- Price, C., Wise, R., & Frackowiak, R. (1996). Demonstrating the implicit processing of visually presented words and pseudowords. *Cerebral Cortex*, 6, 62–70. <https://doi.org/10.1093/cercor/6.1.62>, PubMed: 8670639
- Prinzmetal, W., Treiman, R., & Rho, S. H. (1986). How to see a reading unit. *Journal of Memory and Language*, 25, 461–475. [https://doi.org/10.1016/0749-596X\(86\)90038-0](https://doi.org/10.1016/0749-596X(86)90038-0)
- Protopapas, A., Orfanidou, E., Taylor, J. S. H., Karavasilis, E., Kapnola, E. C., Panagiotaropoulou, G., et al. (2016). Evaluating cognitive models of visual word recognition using fMRI: Effects of lexical and sublexical variables. *Neuroimage*, 128, 328–341. <https://doi.org/10.1016/j.neuroimage.2016.01.013>, PubMed: 26806289
- Purcell, J., Rapp, B., & Martin, R. C. (2021). Distinct neural substrates support phonological and orthographic working memory: Implications for theories of working memory. *Frontiers in Neurology*, 12, 681141. <https://doi.org/10.3389/fneur.2021.681141>, PubMed: 34421789
- Purcell, J., Turkeltaub, P., Eden, G., & Rapp, B. (2011). Examining the central and peripheral processes of written word production through meta-analysis. *Frontiers in Psychology*, 2, 239. <https://doi.org/10.3389/fpsyg.2011.00239>, PubMed: 22013427
- Raczy, K., Urbańczyk, A., Korczyk, M., Szewczyk, J. M., Sumera, E., & Szwed, M. (2019). Orthographic priming in braille reading as evidence for task-specific reorganization in the ventral visual cortex of the congenitally blind. *Journal of Cognitive Neuroscience*, 31, 1065–1078. [https://doi.org/10.1162/jocn\\_a\\_01407](https://doi.org/10.1162/jocn_a_01407), PubMed: 30938589
- Rapp, B. (1992). The nature of sublexical orthographic organization: The bigram trough hypothesis examined. *Journal of Memory and Language*, 31, 33–53. [https://doi.org/10.1016/0749-596X\(92\)90004-H](https://doi.org/10.1016/0749-596X(92)90004-H)
- Rapp, B., & Dufor, O. (2011). The neurotopography of written word production: An fMRI investigation of the distribution of sensitivity to length and frequency. *Journal of Cognitive Neuroscience*, 23, 4067–4081. [https://doi.org/10.1162/jocn\\_a\\_00109](https://doi.org/10.1162/jocn_a_00109), PubMed: 21812571
- Rapp, B., Purcell, J., Hillis, A. E., Capasso, R., & Miceli, G. (2016). Neural bases of orthographic long-term memory and working memory in dysgraphia. *Brain*, 139, 588–604. <https://doi.org/10.1093/brain/aww348>, PubMed: 26685156
- Rayner, K., & Reichle, E. D. (2010). Models of the reading process. *Wiley Interdisciplinary Reviews: Cognitive Science*, 1, 787–799. <https://doi.org/10.1002/wcs.68>, PubMed: 21170142
- R Core Team. (2022). *R: A language and environment for statistical computing*. Vienna, Austria: R Foundation for Statistical Computing. Retrieved from <https://www.R-project.org/>.
- Reich, L., Szwed, M., Cohen, L., & Amedi, A. (2011). A ventral visual stream reading center independent of visual experience. *Current Biology*, 21, 363–368. <https://doi.org/10.1016/j.cub.2011.01.040>, PubMed: 21333539
- Ro, T., Wallace, R., Hagedorn, J., Farné, A., & Pienkos, E. (2004). Visual enhancing of tactile perception in the posterior parietal cortex. *Journal of Cognitive Neuroscience*, 16, 24–30. <https://doi.org/10.1162/089892904322755520>, PubMed: 15006033
- Röder, B., Stock, O., Bien, S., Neville, H., & Rösler, F. (2002). Speech processing activates visual cortex in congenitally blind humans. *European Journal of Neuroscience*, 16, 930–936. <https://doi.org/10.1046/j.1460-9568.2002.02147.x>, PubMed: 12372029
- Rueckl, J. G., Paz-Alonso, P. M., Molfese, P. J., Kuo, W.-J., Bick, A., Frost, S. J., et al. (2015). Universal brain signature of proficient reading: Evidence from four contrasting languages. *Proceedings of the National Academy of Sciences, U.S.A.*, 112, 15510–15515. <https://doi.org/10.1073/pnas.1509321112>, PubMed: 26621710
- Sadato, N., Pascual-Leone, A., Grafman, J., Deiber, M.-P., Ibañez, V., & Hallett, M. (1998). Neural networks for braille reading by the blind. *Brain*, 121, 1213–1229. <https://doi.org/10.1093/brain/121.7.1213>, PubMed: 9679774
- Sanchez-Panchuelo, R. M., Besle, J., Beckett, A., Bowtell, R., Schluppeck, D., & Francis, S. (2012). Within-digit functional parcellation of Brodmann areas of the human primary somatosensory cortex using functional magnetic resonance imaging at 7 tesla. *Journal of Neuroscience*, 32, 15815–15822. <https://doi.org/10.1523/jneurosci.2501-12.2012>, PubMed: 23136420
- Sathian, K. (2016). Analysis of haptic information in the cerebral cortex. *Journal of Neurophysiology*, 116, 1795–1806. <https://doi.org/10.1152/jn.00546.2015>, PubMed: 27440247
- Save, E., & Poucet, B. (2009). Role of the parietal cortex in long-term representation of spatial information in the rat. *Neurobiology of Learning and Memory*, 91, 172–178. <https://doi.org/10.1016/j.nlm.2008.08.005>, PubMed: 18782629
- Schreiber, K., & Krekelberg, B. (2013). The statistical analysis of multi-voxel patterns in functional imaging. *PLoS One*, 8, e69328. <https://doi.org/10.1371/journal.pone.0069328>, PubMed: 23861966
- Schuster, S., Hawelka, S., Hutzler, F., Kronbichler, M., & Richlan, F. (2016). Words in context: The effects of length, frequency, and predictability on brain responses during natural reading. *Cerebral Cortex*, 26, 3889–3904. <https://doi.org/10.1093/cercor/bhw184>, PubMed: 27365297
- Simpson, C. (2013). *The rules of Unified English Braille* (2nd ed.). International Council on English Braille.
- Smith, S. M., Jenkinson, M., Woolrich, M. W., Beckmann, C. F., Behrens, T. E., Johansen-Berg, H., et al. (2004). Advances in functional and structural MR image analysis and implementation as FSL. *Neuroimage*, 23(Suppl. 1), S208–S219. <https://doi.org/10.1016/j.neuroimage.2004.07.051>, PubMed: 15501092
- Stelzer, J., Chen, Y., & Turner, R. (2013). Statistical inference and multiple testing correction in classification-based multi-voxel pattern analysis (MVPA): Random permutations

- and cluster size control. *Neuroimage*, 65, 69–82. <https://doi.org/10.1016/j.neuroimage.2012.09.063>, PubMed: 23041526
- Stilla, R., Deshpande, G., LaConte, S., Hu, X., & Sathian, K. (2007). Posteromedial parietal cortical activity and inputs predict tactile spatial acuity. *Journal of Neuroscience*, 27, 11091–11102. <https://doi.org/10.1523/JNEUROSCI.1808-07.2007>, PubMed: 17928451
- Stoeckel, C., Gough, P. M., Watkins, K. E., & Devlin, J. T. (2009). Supramarginal gyrus involvement in visual word recognition. *Cortex*, 45, 1091–1096. <https://doi.org/10.1016/j.cortex.2008.12.004>, PubMed: 19232583
- Striem-Amit, E., Ovadia-Caro, S., Caramazza, A., Margulies, D. S., Villringer, A., & Amedi, A. (2015). Functional connectivity of visual cortex in the blind follows retinotopic organization principles. *Brain*, 138, 1679–1695. <https://doi.org/10.1093/brain/awv083>, PubMed: 25869851
- Su, L., Fonteneau, E., Marslen-Wilson, W., & Kriegeskorte, N. (2012). Spatiotemporal searchlight representational similarity analysis in EMEG source space. In *2012 second international workshop on pattern recognition in neuroimaging* (pp. 97–100). <https://doi.org/10.1109/PRNI.2012.26>
- Tainturier, M.-J., & Rapp, B. (2003). Is a single graphemic buffer used in reading and spelling? *Aphasiology*, 17, 537–562. <https://doi.org/10.1080/02687030344000021>
- Taylor, J. S., Rastle, K., & Davis, M. H. (2013). Can cognitive models explain brain activation during word and pseudoword reading? A meta-analysis of 36 neuroimaging studies. *Psychological Bulletin*, 139, 766–791. <https://doi.org/10.1037/a0030266>, PubMed: 23046391
- Tian, M., Saccone, E. J., Kim, J. S., Kanjlia, S., & Bedny, M. (2022). Sensory modality and spoken language shape reading network in blind readers of braille. *Cerebral Cortex*, 33, 2426–2440. <https://doi.org/10.1093/cercor/bhac216>, PubMed: 35671478
- Van Orden, G. C., Johnston, J. C., & Hale, B. L. (1988). Word identification in reading proceeds from spelling to sound to meaning. *Journal of Experimental Psychology: Learning, Memory, and Cognition*, 14, 371–386. <https://doi.org/10.1037/0278-7393.14.3.371>, PubMed: 2969938
- Veronelli, L., Ginex, V., Dinacci, D., Cappa, S. F., & Corbo, M. (2014). Pure associative tactile agnosia for the left hand: Clinical and anatomo-functional correlations. *Cortex*, 58, 206–216. <https://doi.org/10.1016/j.cortex.2014.06.015>, PubMed: 25046697
- Vetter, P., Bola, Ł., Reich, L., Bennett, M., Muckli, L., & Amedi, A. (2020). Decoding natural sounds in early “visual” cortex of congenitally blind individuals. *Current Biology*, 30, 3039–3044. <https://doi.org/10.1016/j.cub.2020.05.071>, PubMed: 32559449
- Vogel, A., Church, J. A., Power, J. D., Miezin, F. M., Petersen, S. E., & Schlaggar, B. L. (2013). Functional network architecture of reading-related regions across development. *Brain and Language*, 125, 231–243. <https://doi.org/10.1016/j.bandl.2012.12.016>, PubMed: 23506969
- Vogel, A., Miezin, F. M., Petersen, S. E., & Schlaggar, B. L. (2012). The putative visual word form area is functionally connected to the dorsal attention network. *Cerebral Cortex*, 22, 537–549. <https://doi.org/10.1093/cercor/bhr100>, PubMed: 21690259
- Wang, X., Zhao, R., Zevin, J. D., & Yang, J. (2016). The neural correlates of the interaction between semantic and phonological processing for Chinese character reading. *Frontiers in Psychology*, 7, 947. <https://doi.org/10.3389/fpsyg.2016.00947>, PubMed: 27445914
- Winkler, A. M., Ridgway, G. R., Webster, M. A., Smith, S. M., & Nichols, T. E. (2014). Permutation inference for the general linear model. *Neuroimage*, 92, 381–397. <https://doi.org/10.1016/j.neuroimage.2014.01.060>, PubMed: 24530839
- Woolnough, O., Donos, C., Rollo, P. S., Forseth, K. J., Lakretz, Y., Crone, N. E., et al. (2021). Spatiotemporal dynamics of orthographic and lexical processing in the ventral visual pathway. *Nature Human Behaviour*, 5, 389–398. <https://doi.org/10.1038/s41562-020-00982-w>, PubMed: 33257877
- Yarkoni, T., Barch, D. M., Gray, J. R., Conturo, T. E., & Braver, T. S. (2009). BOLD correlates of trial-by-trial reaction time variability in gray and white matter: A multi-study fMRI analysis. *PLoS One*, 4, e4257. <https://doi.org/10.1371/journal.pone.0004257>, PubMed: 19165335